

# Cosmology with a Primordial Scaling Field

Pedro G. Ferreira<sup>1</sup> and Michael Joyce<sup>2</sup>

<sup>1</sup>*Center for Particle Astrophysics, 301 Leconte Hall, University of California, Berkeley, CA 94720*

<sup>2</sup>*School of Mathematics, Trinity College, Dublin 2, Ireland*

A weakly coupled scalar field  $\Phi$  with a simple exponential potential  $V = M_P^4 \exp(-\lambda\Phi/M_P)$  where  $M_P$  is the reduced Planck mass, and  $\lambda > 2$ , has an attractor solution in a radiation or matter dominated universe in which it mimics the scaling of the dominant component, contributing a fixed fraction  $\Omega_\phi$  (determined by  $\lambda$ ) to the energy density. Such fields arise generically in particle physics theories involving compactified dimensions, with values of  $\lambda$  which give a cosmologically relevant  $\Omega_\phi$ . For natural initial conditions on the scalar field in the early universe the attractor solution is established long before the epoch of structure formation, and in contrast to the solutions used in other scalar field cosmologies, it is one which does not involve an energy scale for the scalar field characteristic of late times. We study in some detail the evolution of matter and radiation perturbations in a standard inflation-motivated  $\Omega = 1$  dark-matter dominated cosmology with this extra field. Using a full Einstein-Boltzmann calculation we compare observable quantities with current data. We find that, for  $\Omega_\phi \simeq 0.08 - 0.12$ , these models are consistent with large angle cosmic microwave background anisotropies as detected by COBE, the linear mass variance as compiled from galaxy surveys, big bang nucleosynthesis, the abundance of rich clusters and constraints from the Lyman- $\alpha$  systems at high redshift. Given the simplicity of the model, its theoretical motivation and its success in matching observations, we argue that it should be taken on a par with other currently viable models of structure formation

PACS Numbers : 98.80.Cq, 98.70.Vc, 98.80.Hw

## I. INTRODUCTION

The past twenty years have seen a tremendous revolution in how we study the origin and evolution of our universe. On the one hand developments in theoretical particle physics have lead to a proliferation of ideas on how high energy physics might have an observable effect on the large scale structure of our universe. On the other hand the increasing quality of astrophysical data has led to firm constraints on what physics is allowed in the early universe. Probably the most impressive example of such an interplay is how the COBE detection [1] has affected the most popular and theoretically explored theory of structure formation, the standard cold dark matter model (SCDM).

The SCDM model brings together the idea of inflation [2–4] and the picture of large scale gravitational collapse [5]. A period of superluminal expansion of the universe would have led to the amplification of subhorizon vacuum fluctuations to superhorizon scales. The net result would be a set of scale invariant, Gaussian perturbations which would evolve, through gravitational collapse, into the structures we see today. The relic radiation bears an imprint of these fluctuations from when the universe recombined. The distribution of galaxies and clusters of galaxies should reflect these fluctuations today. It has been found however that the SCDM model cannot successfully accommodate the data observed on all scales. Matching its predictions to COBE measurements (on large scales) of the microwave background, one finds that the amplitude of fluctuations on  $8h^{-1}\text{Mpc}$  scales (where  $h$  is the Hubble constant today in units of  $100\text{km/s/Mpc}$ ) do not match those observed [6]. To be more specific, if we define the amplitude of mass fluctuations in a sphere of radius  $8h^{-1}\text{Mpc}$ ,  $\sigma_8$ , then COBE normalized SCDM predicts  $\sigma_8 = 1.2$  while the measured value (through cluster abundances) is  $\sigma_8 = 0.6 \pm 0.1$ , a discrepancy by a factor of 2. Further not only the amplitude but also the *scale dependence* of the SCDM model differs from the one measured [7], and there are also a number of problems with the non-linear evolution of baryons and velocities on small scales.

These failings of SCDM have led to attempts to modify it, while keeping its basic features intact. The latter (a simple choice of background cosmological parameters with  $\Omega = 1$  and quantum generation of fluctuations) are associated with its theoretical motivation from inflation. The most prominent candidate theories of structure formation of this type are now a universe with a cosmological constant ( $\Lambda\text{CDM}$ ) [8] and a universe with a fifth of its dark matter component in two families of massive neutrinos (MDM) [9]. Models of structure formation in an open universe (OCDM), for which there is considerable evidence, have also been extensively studied [10]. All these models, once COBE normalized, predict the approximately correct distribution of mass fluctuations. Over the past few years other flat models have been constructed which, like MDM, are more related to our understanding of fundamental particle physics. This is the case of decaying cosmological constant models [12,13] and decaying massive particles [6,14]. Unfortunately, unlike the SCDM scenario, all these models involve a tuning of parameters which is unnatural from the point of view of

particle physics, simply because one is using super-GeV physics to explain sub-eV observations. Just as is the case of  $\Lambda$ CDM (which involves tuning the cosmological constant to be relevant only at present epochs) this tuning does not provide a reason to discard these models, but is a very unattractive feature of them.

Both the cosmology of weakly coupled scalar fields and their theoretical motivation have been much studied since the advent of the idea of inflation. In most of the theoretical particle physics extensions of the standard model (e.g. supersymmetry and supergravity) weakly coupled scalar fields of various kinds are ubiquitous. Unfortunately there is as yet no experimental evidence for the existence of any fundamental scalar field at all, in particular the Higgs particle of the standard model remains to date undetected. However the theoretical motivation for such scalar fields is sufficiently compelling that it is certainly worthwhile considering what consequences their existence might have for cosmology beyond the confines of inflation. An example of this is given by the main alternative of structure formation - defect theories - which usually involve the existence of some scalar field e.g. the ‘texture’ theory [15] relies on the existence of a scalar field invariant under a global non-abelian symmetry broken at the GUT scale, with associated goldstone particles which are unobservably weakly coupled to ordinary matter.

The role that a weakly coupled scalar field might play in late time cosmology if it contributes a component to the homogeneous background energy density of the universe has also been investigated. In [16] the authors considered in general terms the idea that a significant contribution to the energy density from a homogeneous scalar field could have an important effect on structure formation, and applied the idea to a baryonic universe with a initial spectrum of perturbations with power law behaviour. After some general analysis of the homogeneous dynamics, the model singled out for a detailed treatment was that of a scalar field in a negative power law potential which comes to dominate at late times, producing behaviour very similar to that associated with a cosmological constant. Another kind of model which has been developed in detail, for the case of a cold dark matter dominated cosmology, in [12,13] involves a cosine potential with a combination of Planck and sub eV physics. This provides a specific realisation of a ‘decaying cosmological constant’, in which the field initially behaves like a cosmological constant and then rolls so that it scales asymptotically like matter. All these models have an energy density in the scalar field which comes to dominate at late times, as have two more recent very detailed studies [17,18]. In [17] the case of a scalar field which scales slower than matter is described more generically in terms of its equation of state, and in [18] the specific cases of late time dominance realized in both cosine and exponential potentials.

In this paper we present in detail the results which have been reported in [19]. The model we study is SCDM with the addition of a scalar field  $\Phi$  with a simple exponential potential  $V = M_P^4 \exp(-\lambda\Phi/M_P)$  where  $M_P \equiv (8\pi G)^{-\frac{1}{2}} = 2.4 \times 10^{18} \text{GeV}$  is the reduced Planck mass, and  $\lambda > 2$ . In this specific case there is a very special and interesting solution for matter and radiation coupled through gravity to this field, in which the scalar field energy follows that of the dominant component, contributing a fixed fraction of the total energy density determined by  $\lambda$ . The existence of this homogeneous solution was shown in [16,20,21]. Because the scalar field can contribute at most a small fraction of the total energy density at nucleosynthesis, its potential interest in the context of the problem of structure formation has been overlooked. This constraint suggests *prima facie* that the field in such an attractor can have little effect on cosmology at late time. As we shall see, this is incorrect, for the simple reason that a small contribution acting over a long time can have as big an effect as a large contribution entering only at late times. The particular merit of the model is related to the fact that the cosmological solution is an attractor for the scalar field: Because of this, there is no tuning of the type involved in *all* other proposed modifications of SCDM. The only parameter additional to SCDM is  $\lambda$ , and the value ( $\sim 5 - 6$ ) which gives a best fit to structure formation, is of the order naturally expected in the particle physics models in which the potential arises. As a cosmology it resembles MDM much more than any of the scalar field models which have been studied in the literature.

Some comment is perhaps necessary at the outset regarding the assumption that the universe is flat and dominated by a component scaling as matter, as there is mounting observational evidence that this is not the case. The most advertised is the age problem, that is, the fact that we see objects which are older than the age of the universe if we assume a flat matter dominated universe with the currently observed Hubble constant of  $H_0 = 65 \pm 10 \text{kms}^{-1} \text{Mpc}^{-1}$ . Several of the modifications we have discussed (in particular the cosmological constant model and some of the scalar field models) avoid this problem since the dominant component at the present epoch is not matter. The recent measurements of the Hipparcos satellite [22] seem to indicate that the age of these objects have been overestimated by around 10% and a re-analysis of the uncertainties in the estimates seem to indicate that a flat matter dominated universe with  $H_0 < 66 \text{kms}^{-1} \text{Mpc}^{-1}$  is compatible with the current age estimates. Another argument for a low density universe comes from the analysis of large scale flows. In [23] it has been argued that  $\beta = \Omega^{0.6}/b < 1$  from the analysis of the MARK III data and comparison with the IRAS surveys. However there is concern with the self consistency of the velocity data and another group [24] indicates that the the flows are consistent with a universe with  $\Omega = 0.4 - 1$ . Small scale observations also seem to indicate that there are problems with a high density universe. In particular the baryon fraction in clusters is difficult to reconcile with the BBN limits unless one considers a low density universe [26]. Again there are uncertainties in such an analysis; they rely on elaborate numerical simulations which are at the limit

of current computational power. It is conceivable that some physics (such as cooling of the cluster medium) is being overlooked. The same can be said for the cold velocity dispersion which is measured on few Mpc scales [5]. Although all these observations together begin to make a strong case for an open universe, the uncertainties and inconsistencies are sufficiently large for us to still consider a high density, matter dominated universe. It may be that in the next few years the evidence is sufficiently compelling to rule out these models, but this is definitely not the case yet.

The structure of the paper is as follows. In section II we first discuss the homogeneous modes of scalar fields in a universe with matter and radiation in general terms, and explain how the case of a simple exponential with its attractor solutions for  $\lambda > 2$  is a special one. We discuss briefly the possible origin of exponential potentials in fundamental theories. We then discuss the initial conditions on this scalar field in the early universe, and when these lead the attractor to be established. In typical inflationary theories we argue that the attractor describes the homogeneous cosmology well before nucleosynthesis, while in an alternative theory of reheating which can be realised with the same exponential field the scalar field may still be negligible at nucleosynthesis for natural parameter values. In section III we analyse the evolution of perturbations in our scenario. We describe the complete set of equations which govern their evolution and analyse the asymptotic behaviour in the interesting regimes. The similarities with evolution of density fluctuations in an MDM universe lead us to pursue the comparison in some detail and we come to the conclusion that scalar field is more effective at suppressing perturbations than hot dark matter. We also consider the effect on the cosmic microwave background (CMB) and deconstruct the different effects it has on the angular power spectrum of the CMB. In section IV we compare the predictions of linear perturbation theory (using the full Boltzmann-Einstein equations) with some observations. In particular we compare it to the COBE data and then use this comparison to normalize the theory and compare to the Peacock and Dodds data. As a byproduct we derive a fit to  $\sigma_8$  for our models and we quantify the amount of structure on small scales and high redshift, comparing with constraints derived from Lyman- $\alpha$  systems. In V we summarise our findings and draw some conclusions about future prospects for our model and other issues related to it which might be further investigated.

## II. THE ‘SELF-TUNING’ SCALAR FIELD WITH AN EXPONENTIAL POTENTIAL

In this section we describe in detail the homogeneous attractor solutions which specify the zero-order cosmology, about which we treat perturbations fully in the subsequent part of the paper. We explain the very special feature of this model which contrasts it with other scalar field cosmologies which have been treated in the literature: *No special energy scale characteristic of late time cosmology need be invoked to produce the required solution.* We will show that for a very wide and natural range of initial conditions on the scalar field in the very early universe, the attractor will be attained as early as assumed in the rest of the paper.

### A. Scaling of the Energy Density in a Scalar Field

We begin with a general discussion of homogeneous FRW cosmology in which there is, in addition to the usual matter and radiation content, a contribution to the energy momentum coming from a scalar field  $\Phi$  with a potential  $V(\Phi)$ . In the rest of the paper we use the notation  $\Phi = \phi + \varphi$ , where  $\varphi$  denotes the perturbation about the homogeneous solution  $\phi$ . Working for the moment in comoving coordinates in which the metric is  $ds^2 = -dt^2 + a^2\delta_{ij}dx^i dx^j$  (where  $a$  is the scale factor), the contribution to the energy-momentum tensor from the scalar field is

$$T_{00} = \rho_\phi \quad T_{ij} = a^2 p_\phi \delta_{ij} \quad \text{where} \quad \rho_\phi = \left[ \frac{1}{2} \dot{\phi}^2 + V(\phi) \right] \quad p_\phi = \left[ \frac{1}{2} \dot{\phi}^2 - V(\phi) \right]. \quad (1)$$

The equations of motion for the scalar field are then

$$\ddot{\phi} + 3H\dot{\phi} + V'(\phi) = \frac{1}{a^3} \frac{d}{dt}(a^3 \dot{\phi}) + V'(\phi) = 0 \quad (2)$$

$$H^2 = \frac{1}{3M_P^2} \left( \frac{1}{2} \dot{\phi}^2 + V(\phi) + \rho_n \right) \quad (3)$$

$$\dot{\rho}_n + nH\rho_n = 0 \quad (4)$$

where  $\rho_n$  is the energy density in radiation ( $n = 4$ ) or non-relativistic matter ( $n = 3$ ),  $H = \frac{\dot{a}}{a}$  is the Hubble expansion rate of the universe, dots are derivatives with respect to time, primes derivatives with respect to the field  $\phi$ , and  $M_P \equiv (8\pi G)^{-\frac{1}{2}} = 2.4 \times 10^{18} \text{GeV}$  is the reduced Planck mass. The scalar field is assumed to be coupled to ordinary matter only through gravity. Multiplying (2) by  $\dot{\phi}$  and integrating, one obtains

$$\rho_\phi(a) = \rho(a_o) \exp\left(-\int_{a_o}^a 6(1-\xi(a))\frac{da}{a}\right) \quad \text{where} \quad \rho_\phi = \frac{1}{2}\dot{\phi}^2 + V(\phi) \quad \xi = \frac{V(\phi)}{\rho_\phi}. \quad (5)$$

It follows from this that, given the range of possible values  $0 < \xi < 1$  (assuming  $V(\phi)$  is positive), the energy density of a scalar field has the range of scaling behaviours

$$\rho_\phi \propto 1/a^m \quad 0 \leq m \leq 6 \quad (6)$$

How the energy in a homogeneous mode of a scalar field scales is thus determined by the ratio of the potential to the kinetic energy. Alternatively one can phrase the statement in terms of the equation of state obeyed by the mode: From (1) we have  $\xi = \frac{1}{2}(1-w)$  where  $p_\phi = w\rho_\phi$ , and  $m = 3(1+w)$  (for constant  $w$ ) in (5).

These statements are true independent of any specific assumption about  $H$  i.e. about what dominates the energy density of the universe. When the potential energy dominates over kinetic energy, we have  $\xi \rightarrow 1$  and therefore  $\rho_\phi \approx \text{constant}$  i.e. an energy density which behaves like a cosmological constant (and  $w = -1$ ); in the opposite limit of  $\xi \rightarrow 0$  i.e. a kinetic energy dominated mode, we have an energy density with  $\rho_\phi \propto 1/a^6$  i.e. red-shifting faster than radiation or matter (and  $w = +1$ ). Inflation occurs when the former type of mode also dominates the energy density; the opposite limit, when the universe is dominated by the kinetic energy of a scalar field (which, following [44], we refer to as *kination*) gives a sub-luminal expansion with  $a \propto t^{\frac{1}{3}}$ .

We now consider more specifically what sorts of potentials give rise to these different types of scaling. One simple case to analyse is that in which a field rolls about the minimum of a potential. In such an oscillatory phase the approximate scaling of the energy density can be extracted from (5) by replacing  $\xi$  by its average value over an oscillation. For a potential which is power law about its minimum with  $V(\phi) \propto \phi^n$  the result [27] is that

$$\xi = \frac{2}{n+2} \quad \rho_\phi \propto 1/a^m \quad m = \frac{6n}{n+2} \quad (7)$$

reproducing the well known result that a coherent mode oscillating in a quadratic potential gives the same scaling as matter, and a  $\phi^4$  potential that of radiation. For  $n > 4$  one obtains modes scaling faster than radiation.

Again this statement does not depend on what component dominates the energy density, and the same scaling applies to the mode irrespective of whether the universe has  $\rho_n = 0$ , or is matter or radiation dominated. The case of a field rolling down a potential (before it reaches its minimum, or if it has no minimum) is quite different. The equation of motion (2) is just a damped roll with the energy content determining the damping through (3). The scaling obtained for a given potential depends on what components are present, because what determines the scaling is the balance between the increase in kinetic energy relative to potential energy as the field rolls down the potential, and the decrease of the same quantity due to the damping. The criterion for a particular scaling is therefore a requirement of the ‘steepness’ of the potential. That the simple exponential potential  $V(\phi) = V_o e^{-\lambda\phi/M_P}$  provides the appropriate yard-stick in the case of scalar field domination is indicated by the existence of a family of solutions for this potential to (2)-(3) with  $\rho_n = 0$  [16,20,21]

$$\phi(t) = \phi_o + \frac{2M_P}{\lambda} \ln(tM_P) \quad \phi_o = \frac{2M_P}{\lambda} \ln\left(\frac{V_o\lambda^2}{2M_P^4(6-\lambda^2)}\right) \quad \xi = 1 - \frac{\lambda^2}{6} \quad \rho_\phi \propto \frac{1}{a^{\lambda^2}} \quad a \propto t^{2/\lambda^2} \quad (8)$$

for  $\lambda < \sqrt{6}$ , and  $\phi_o$  can always be chosen to be zero by redefining the origin of  $\phi$ , in which case  $V_o = \frac{2}{\lambda^2}(\frac{6}{\lambda^2} - 1)M_P^4$ . These solutions, which are attractors<sup>1</sup> were written down [28,29] in the context of power-law inflation [30], associated with the superluminal growth of the scale-factor for  $\lambda < \sqrt{2}$ . For  $\lambda > 6$  there is not a single attractor with a finite value of  $\xi$ , but every solution has  $\xi \rightarrow 0$  asymptotically and  $\rho \propto 1/a^6$ .

As  $\lambda$  increases from zero we obtain the entire range of possible scaling behaviours (6) for the energy in a scalar field. By comparison with this potential we can infer how scalar modes will scale: The ‘slow-roll’ conditions ( $|M_P V'/V| \ll \sqrt{6}$ ,  $|M_P^2 V''/V| \ll 3$ ) for inflation, for example, could be stated as the requirement that the first two derivatives of a potential be smaller than those of an exponential with  $\lambda = \sqrt{3}$ . An analogous ‘fast-roll’ condition for ‘kination’ can clearly be provided by comparison with an exponential with  $\lambda = \sqrt{6}$  e.g. a potential  $\sim e^{-\mu\phi^2/M_P^2}$  will have such modes for sufficiently large  $\phi$ .

These statements apply only to the case of scalar field dominance since we took  $\rho_n = 0$ . What interests us in the present context is how the scalar energy behaves in the presence of matter and radiation i.e. with  $\rho_n \neq 0$ . There are

---

<sup>1</sup>It is simple to verify directly from (2) and (3) that homogeneous perturbations about the solution decay as  $t^{-1}$  and  $t^{1-\frac{6}{\lambda^2}}$ .

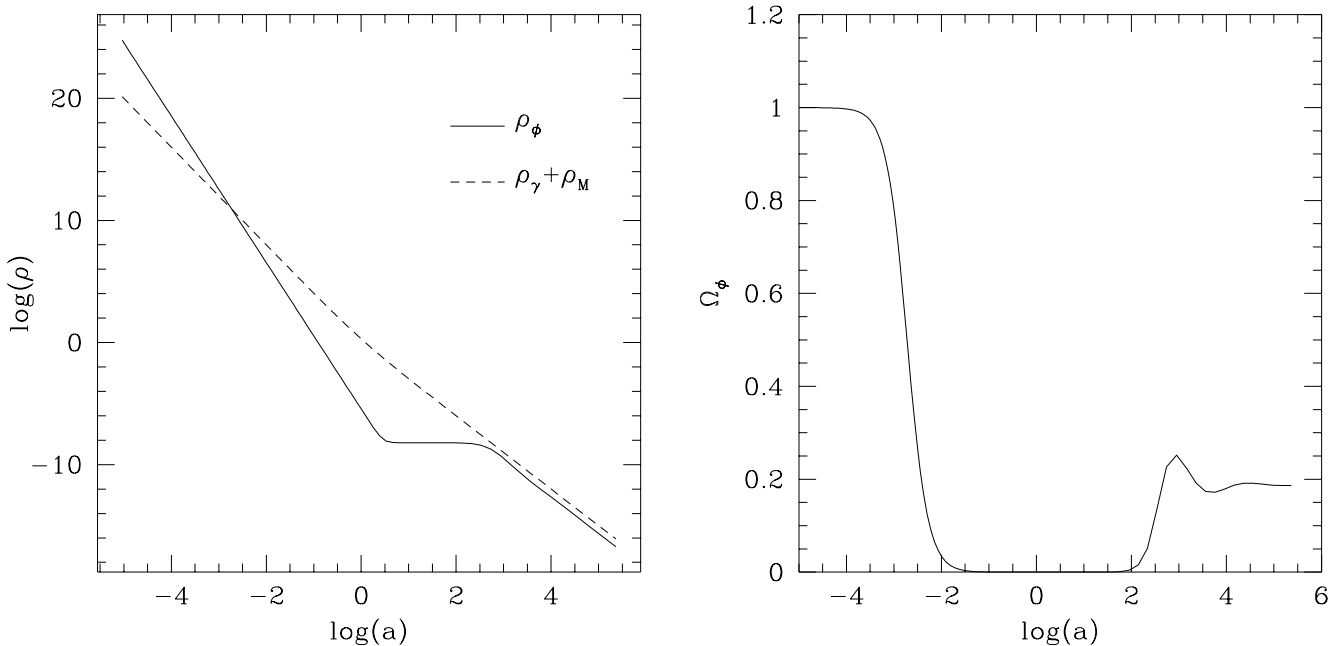


FIG. 1. In the left panel we plot the evolution of the energy density in the scalar field ( $\rho_\phi$ ) and in a component of radiation-matter as a function of scale factor for a situation in which the scalar field (with  $\lambda = 4$ ) initially dominates, then undergoes a transient and finally locks on to the scaling solution. In the right panel we plot the evolution of the fractional density in the scalar field.

two quite distinct cases which can be immediately distinguished according to their behaviour when  $\rho_n = 0$ : Those potentials in which the energy density scales slower than  $1/a^n$  (i.e.  $\lambda < \sqrt{n}$ ), and those in which it scales faster ( $\lambda > \sqrt{n}$ ). When  $\rho_n \neq 0$  these two types of potential will show very different behaviour for the following reason: Adding a component increases the damping term in (2), and it follows that the scaling with  $a$  of the energy density in the scalar field is always *slower* i.e.  $\rho_\phi \propto 1/a^{\lambda^2 - \delta}$  with  $\lambda^2 \geq \delta \geq 0$ . For  $\lambda < \sqrt{n}$  the scalar energy will still red-shift slower than the other component and it will always come to dominate asymptotically, approaching the attractor (8). For  $\lambda > \sqrt{n}$ , however, the scalar field energy cannot always scale as in the case  $\rho_n = 0$ . By doing so it would become arbitrarily sub-dominant relative to the component  $\rho_n$ , and thus arbitrarily strongly damped. Eventually this damping must reduce its kinetic energy so that it will then scale slowly (since  $\xi \rightarrow 1$ ) and begin to catch up again with the  $\rho_n$  component. It is not surprising then to find that there are in fact, for  $\rho_n \neq 0$ , a quite different set of solutions to (2)-(4) for the exponential potential [16,20], in which the energy in the scalar field mimics that of the dominant component, contributing a fixed fraction of the energy density determined by  $\lambda$  given by

$$\Omega_\phi \equiv \frac{\rho_\phi}{\rho_\phi + \rho_n} = \frac{n}{\lambda^2} \quad \rho_\phi \propto 1/a^n \quad \xi = 1 - \frac{n}{6} \quad (9)$$

This solution is also an attractor [21], with  $\phi$  again evolving logarithmically in time as given by (8) (with only  $\phi_o$  differing). Fig 1 illustrates the evolution towards the attractor starting from initial conditions with the scalar field energy very dominant (obtained by a numerical evolution of the homogeneous equations of motion for the exponential scalar field with  $\lambda = 4$  and components of radiation and matter which are equal at  $a = 1$ ). The scalar field energy first scales rapidly, approximately as  $1/a^6$  as indicated by the solution (8), until it has undershot the energy density in the radiation. It then turns around and starts scaling much slower than radiation or matter until it again catches up with them in the matter dominated regime, and then settles down at the fraction given by (9) with  $n = 3$ . As anticipated above the main feature - the turn around in the scaling - can be understood to arise from the increase in damping as the radiation/matter becomes dominant. One can easily see quantitatively how this comes about: The energy scaling as  $1/a^6$  scaling occurs while the  $V'(\phi)$  term in (2) is very subdominant and we have then  $\dot{\phi} \propto 1/a^3$ . If the dominant component on the RHS of (2) is radiation/matter one then obtains the evolution of the field

$$\begin{aligned} \phi(t) &= \phi_o + \dot{\phi}_o t_o \left(1 - \left(\frac{t_o}{t}\right)^2\right) & \rho_n \ll \rho_\phi \quad (n = 3) \\ \phi(t) &= \phi_o + 2\dot{\phi}_o t_o \left(1 - \left(\frac{t_o}{t}\right)^{\frac{1}{2}}\right) & \rho_n \ll \rho_\phi \quad (n = 4) \end{aligned} \quad (10)$$

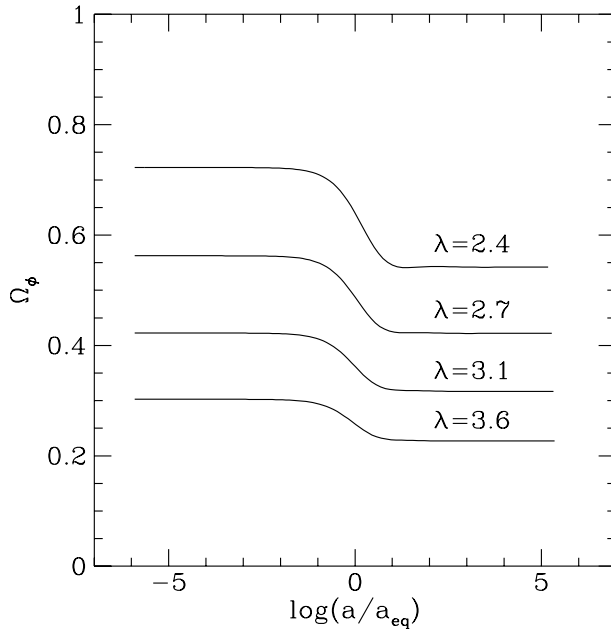


FIG. 2. The evolution of the fractional energy density in the scalar field for a selection of  $\lambda$ s

In contrast to the case of the logarithmic dependence on time of the attractors, the potential term evolves in either case more slowly than the first two terms in (2). This results in a slow-down in the scaling of the scalar energy which drives it back eventually towards the dominant component. We will discuss in greater detail below what determines the duration of this transient period in which the scalar energy is very sub-dominant. We will also see below that the re-entry in this example in the matter-dominated epoch is just a result of the initial conditions. For  $\lambda > 2$  the attractor exists both in the radiation and matter dominated epochs. Given that the relative contribution of the scalar field energy and the dominant component differs so little in the two epochs (by a factor of 3/4) one would anticipate that the scalar field, if established in the attractor in the radiation dominated epoch will match tightly onto its asymptotic value in the matter dominated epoch. That this is indeed the case can be seen from Fig 2, which shows the evolution of the fractional contribution to the energy density for a range of values of  $\lambda$  (with the scalar field prepared in the attractor at the beginning of the evolution).

The conclusion from this discussion is that, in the presence of matter or radiation, a scalar potential which is flatter than a simple exponential with  $\lambda = \sqrt{3}$  will support modes with energy scaling slower than matter, and always asymptotically dominate. Simple exponentials with  $\lambda < 2$  have attractors in the radiation and matter dominated epoch given by (9), and those with  $\sqrt{3} < \lambda < 2$  in the matter dominated epoch only. A scalar field rolling down a potential steeper than these simple exponential e.g.  $\sim e^{-\mu\phi^2/M_P^2}$  will clearly always decay away asymptotically relative to radiation/matter. We also saw that oscillating modes scale in a way which is independent of what other component is present, and there are no attractor solutions.

The attractor solutions for the exponential scalar field are therefore a special case. Before embarking on the full treatment of the cosmology in which the attractor (9) describes the unperturbed limit, we discuss further why this attractor solution is particularly interesting from a cosmological point of view: By virtue of its being an attractor, it avoids the tuning problems which are inevitably a feature of all other scalar field cosmologies which have been proposed. First, however, we discuss briefly another attractive aspect of the required potentials.

## B. Theoretical Origin of Exponential Potentials

Scalar fields with simple exponential potentials occur in fact quite generically in certain kinds of particle physics theories. Because of the existence of the power-law inflationary solutions (8) such theories have been studied in some detail by various authors, with attention focussed on models and parameters which lead to inflation. We will not carry out any detailed analysis here of particular theories which would produce the exact parameters required for the present case, but limit ourselves to a brief review of such theories and the observation that the parameter values which we require are quite reasonable in the context of such theories.

The first are Kaluza-Klein theories in which the fundamental theory has extra dimensions, which are compactified to produce the four dimensional world we observe. In the effective four dimensional theory scalar fields arise which correspond to the dynamical degree of freedom  $L$  associated with the ‘stretching’ of the internal dimensions. The potential is generically exponential because the kinetic term has the form  $(\dot{L}/L)^2$ , while the potential ‘stretching energy’ is polynomial in  $L$ . A simple example [32,34] is a six-dimensional Einstein-Maxwell theory where the two extra dimensions are compactified to  $S^2$  with radius  $L$ . Defining a field  $\Phi$

$$\Phi = 2M_P \ln L \quad (11)$$

results simply in four-dimensional Einstein gravity minimally coupled to this field which then has the potential

$$V(\Phi) \propto \exp\left(-\frac{\Phi}{M_P}\right) \left[1 - \exp\left(-\frac{\Phi}{M_P}\right)\right]^2 \quad (12)$$

In the regime of large  $\Phi$  we have  $V(\Phi) \sim \exp(-\frac{\Phi}{M_P})$  i.e. effectively a simple exponential potential with  $\lambda = 2$ . Another example studied in detail in [31–33] is the case of a pure gravitational theory with higher derivative terms in an arbitrary number of dimensions,  $D+4$ , where spontaneous compactification arises because of the higher derivative terms. The effective four dimensional theory is in this case considerably more complicated, but again includes a scalar field  $\Phi$  defined as the logarithm of the ‘radius’ of the compactified  $D$ -dimensions which gives, in certain regimes, a potential driving the dynamics of the zero mode of the field of the form of (2) with  $V(\Phi) \sim \exp(-D\frac{\Phi}{\sqrt{8\pi}M_P})$ .

Another set of models in which such potentials appear is in supergravity and superstring theories [35]. One of the most studied is the Salam-Sezgin model with,  $N = 2$  supergravity coupled to matter in six dimensions. It predicts [28] the existence of two scalar fields  $\Phi$  and  $\Upsilon$  with a potential of the form

$$V(\Phi, \Upsilon) = \bar{V}(\Upsilon) \exp(-\sqrt{2}\frac{\Phi}{M_P}) \quad (13)$$

For  $\Upsilon \gg 0$  it corresponds to a potential of the required form we want, with  $\lambda = \sqrt{2}$ . Further examples relevant to inflation are given by the authors of [36], who find two scalar fields with  $\lambda = \sqrt{2}$  and  $\lambda = \sqrt{6}$  in an  $N = 2$  model, as well as in an  $N = 1$  ten-dimensional model with gaugino condensation [37].

A further class of theories in which such fields arise is in higher order gravity. There is a conformal equivalence (see [38], and references therein) between pure gravity described by a lagrangian which is an analytic function of the scalar curvature  $R$  and general relativity plus a scalar field with a determined potential, and in the presence of matter the metric associated with the latter description is the physical one [39]. For example [38] in  $d$  dimensions the potential in the case of a lagrangian quadratic in  $R$  is

$$V(\Phi) \propto \exp\left(\frac{d-4}{2}\frac{\Phi}{M_P}\right) \left[1 - \exp\left(-\frac{d-2}{2}\frac{\Phi}{M_P}\right)\right]^2 \quad (14)$$

and, for  $d = 4$  and a polynomial lagrangian of the form  $\sum_{n=1}^k a_n R^n$ , it is

$$V(\Phi) = A_1 \exp\left(-2\frac{\Phi}{M_P}\right) + \sum_{n=2}^k A_n \exp\left(-2\frac{\Phi}{M_P}\right) \left[1 - \exp\left(\frac{\Phi}{M_P}\right)\right]^n \quad (15)$$

where the  $A_n$  are rational coefficients determined by the  $a_n$ . As  $\Phi \rightarrow +\infty$  we have  $V \sim \exp[(k-2)\Phi/M_P]$ .

All previous analysis of the cosmological consequences of the existence of such scalar fields has focussed on inflation, which is realized in the case of the simple exponential for  $\lambda < \sqrt{2}$ . The fact that many of these models can at best give  $\lambda \lesssim \sqrt{2}$  rather than the considerably flatter potentials needed for inflation (to naturally give a large number of e-foldings and a nearly flat spectrum of perturbations) meant that these theories provided a general motivation rather than a realistic model. In [36], for example, an extra ad hoc damping term was introduced to produce a more satisfactory model from supergravity motivated models. In the present context this is not the case: We will see that the most interesting range for structure formation is  $\Omega_\phi \in [0.08, 0.12]$  in the matter era which approximately corresponds to the range  $\lambda \in [5, 6]$ . Although these values are a little larger than in the simplest models we have reviewed, some of the models above clearly can lead to parameters in this range, and, for example, the number of compactified dimensions required to give these values in the first type of theory we reviewed is certainly not unreasonable in the context of superstring theory. In terms of the theoretical origin of the potential we study therefore, it is not just the form of the potential which is one which arises naturally, but it may also be that the precise value of the single free parameter in this potential is a natural one. Clearly further analysis of such models would be required to make a stronger statement than this, and to see if the cosmological effect of these fields which we study in this paper might ultimately be used to give us specific hints about fundamental particle physics.

### C. Nucleosynthesis Constraints

In considering the possibility that some significant fraction of the energy density of the universe may be in a homogeneous mode of a scalar field, the earliest constraint comes from nucleosynthesis. Such a contribution from a weakly coupled scalar field enters in determining the outcome of nucleosynthesis (the primordial densities of the light nuclei) only through the expansion rate. Adding a component increases the expansion rate at a given temperature. The dominant effect of such a change is in its effect on the ratio of neutrons to protons when the weak interactions keeping them in equilibrium freeze-out at a temperature of  $\sim 1\text{MeV}$ . The range of expansion rates at this temperature compatible with observations is usually translated into a bound on the number of effective relativistic degrees of freedom at  $\sim 1\text{MeV}$ . Taking  $\Delta N_{eff}$  to be the maximum number of such degrees of freedom additional to those of the standard model (with three massless neutrinos) the equivalent bound on the contribution from a scalar field is

$$\Omega_\phi(1\text{MeV}) < \frac{7\Delta N_{eff}/4}{10.75 + 7\Delta N_{eff}/4}, \quad (16)$$

(where 10.75 is number of effective degrees of freedom in the standard model). A wide range of values for the upper bounds on  $\Delta N_{eff}$  exists in the literature, the variation being due both to the data taken into account and the methods of analysis used. We will not attempt here to review all the issues involved and accept one or other bound as definitive (see, for example, [43] for a full discussion). The tendency in the last few years has been towards less restrictive bounds than were generally thought correct previously. A typical value now used is a bound of  $\Delta N_{eff} = 0.9$  which is given by various authors [40], or even a more conservative one of  $\Delta N_{eff} = 1.5$  by others [41,42]. This range corresponds here to

$$\Omega_\phi(1\text{MeV}) < 0.13 - 0.2 \quad (17)$$

This is the range of values we will take when we discuss nucleosynthesis in the rest of the paper. The result for more restrictive nucleosynthesis analyses can be read off from (16). Note also that we have assumed here that the standard model number of relativistic degrees of freedom at 1MeV. The strict experimental lower bound on this number is in fact 9, given that the upper bound on the mass of the  $\tau$  neutrino is 18 MeV [25]. In the case that the  $\tau$  neutrino is non-relativistic (and decays before nucleosynthesis) the bound (17) is changed to  $\Omega_\phi(1\text{MeV}) < 0.27 - 0.33$ .

### D. Scalar Fields at Late Time and Fine-Tuning

In modifications of standard inflationary flat cosmologies [16–18] involving a contribution from a scalar field which have been considered to date, attention has been focussed exclusively on the case that the scalar field contributes significantly only at recent epochs, at the earliest well after the transition to matter domination. The main reason for this is that one of the motivations for many models has been to produce a contribution at late times which scales slower than matter and dominates asymptotically, producing effects very similar to that of a cosmological constant. In this case there is unavoidably the same sort of tuning as involved in the cosmological constant model: One requires an initial energy density in the scalar field which is characterised by the energy density in the universe at recent epochs.

Another kind of model which has been considered is that in which the energy density in the scalar field scales like matter asymptotically, implemented in an oscillating mode of a sinusoidal potential. If the field lies initially away from the minimum, it becomes important once the curvature of the potential is comparable to the expansion rate and initially behave like a cosmological constant before rolling down the potential and scaling asymptotically like matter. This model also involves the same sort of tuning, since a small energy scale must be introduced to single out this late time at which the scalar field becomes dynamically important. It has been argued in [12] that there are particle physics motivations for the introduction of such a potential with such a characteristic scale, and that there is nothing ‘unnatural’ about models of this type.

The special case we have discussed of the attractor in the exponential potential is quite different, simply because it is an attractor. In contrast the only attractor in the case of a field asymptotically scaling slower than matter is the pure scalar field dominated cosmology, and the tuning referred to is just that required to make the coupled system of scalar field and matter approach this attractor just at the present epoch. For the models with an oscillating mode there is no attractor, and the tuning consists in fixing the energy density in the scalar field to be comparable to that in matter when it starts scaling like matter. With the attractor for matter and radiation in the present case, the scalar field plus matter/radiation will always end up in this solution asymptotically. In this paper we will take this solution to apply from the beginning of our simulation of structure formation, deep in the radiation era at a red-shift of  $z \sim 10^7$  when the temperature is  $\sim 100\text{eV}$ . We now address the question as to what range of initial conditions



on the scalar field in the early universe will give rise to this behaviour. In the course of this analysis we will also determine what sorts of initial conditions are compatible with the late entry (in the matter era at a red-shift of  $\sim 70$ ) to the attractor discussed in [18].

### E. Initial Conditions in the Early Universe and the ‘Self-Tuning’ Scalar Field

The assessment of what are ‘natural’ initial conditions for a scalar field in the early universe requires of course a particular framework within which to address the question. What we need to determine is essentially just the kinetic and potential energy in the scalar field at some early time relative to that in radiation (and therefore matter). Given that we are working in the context of inflation-motivated flat homogeneous cosmologies (and will assume Gaussian adiabatic perturbations of the type produced by inflation) we assess the question within this framework. The energy density in radiation is then determined by how the universe is reheated after inflation. We consider both the usual scenario for reheating by decay of the inflaton and then an alternative scenario introduced in [47]. The reason for our detailed analysis of this second non-standard case will become clear below.

First consider the standard reheating scenario. We suppose there is an inflaton field and the scalar field with an exponential potential  $V_o e^{-\lambda\phi/M_P}$  with  $\lambda > 2$  (i.e. with the attractor in the radiation/matter epochs which we will consider). Let us consider a typical inflationary model e.g. chaotic inflation. The simplest and most natural assumption for the relative energy densities at the onset of inflation is

$$\frac{1}{2}\dot{\phi}^2 \sim V(\phi) \lesssim V_{inf} \quad (18)$$

where  $V_{inf}$  is the energy density in the inflaton. We make the latter assumption since it is required for the onset of inflation. The dynamics of the two fields are then described by the equations (2)-(4), but with  $\rho_n$  now the total energy of the inflaton and  $n$  a function of the inflaton  $n = 6(1 - \xi_{inf})$ , where  $\xi_{inf}$  is the ratio of the potential energy of the inflaton to its total energy. For the same reasons as in the case discussed above when  $\rho_n$  describes matter or radiation, there is an attractor solution given by (9) with  $n = 6(1 - \xi_{inf})$  (assuming  $n$  changes slowly which is the case for slow-roll inflation). The energy in the scalar field scales so slowly because its roll is strongly damped by the inflaton, with (9) specifying the exact ratio of energies at which the damping slows the roll to give precisely the same scaling as for the inflaton. In inflation driven by an exactly constant energy density, this ratio is zero and just represents the asymptotically approached solution in which the scalar field rolls away to an arbitrarily large values of the field after an arbitrarily long time. In any realistic model of inflation however the inflaton must roll in a non-trivial potential in order to exit from inflation and  $\xi_{inf} \neq 1$ . For example, in chaotic inflation in a potential  $\sim \phi_{inf}^4$ , one has, in the slow-roll inflationary regime,  $n = \frac{8}{3}(\frac{M_P}{\phi_{inf}})^2$ . Once inflation commences, say at  $\phi_{inf} = \phi_{inf}^o$ , the energy in the scalar field will be driven towards

$$\Omega_\phi^o = \frac{n_o}{\lambda^2} = \frac{8\Omega_\phi^m}{9} \left(\frac{M_P}{\phi_{inf}^o}\right)^2 \approx \frac{\Omega_\phi^m}{9N_e} \quad (19)$$

where  $\Omega_\phi^m$  is the fraction of the energy density in the attractor in the matter era, and  $N_e \approx \frac{1}{8}(\frac{\phi_{inf}^o}{M_P})^2$  is the number of e-foldings of inflation. As the inflaton rolls down the potential  $n$  increases and the fraction of energy in the attractor grows.

Starting from initial conditions like (18) the roll of the scalar field is very rapidly over-damped due to the rapid red-shifting of its initial energy density. It will always then scale much slower than it would in the absence of the inflaton, with  $\xi \approx 1$ . In the next section we will see that this is enough to ensure that its energy density relative to the inflaton will never drop substantially below that in the attractor. (The transient with sub-dominance we observe in that case results from the field having initially evolved without the  $\rho_n$  component playing any role for a long period). Without analysing in detail how precisely the energy density can track the (growing) attractor value during inflation, we thus conclude that the fraction of the energy in the scalar field at the end of inflation will be bounded below by  $\Omega_\phi^o$  as given by (19).

From Fig 3 (and our previous discussion of Fig 1) we see that this conclusion is enough to establish that, after inflation, the attractor for the scalar field in the radiation dominated epoch is approached within a few expansion times of the end of inflation. When the inflaton starts oscillating and/or decays it begins to scale like matter or radiation, while the scalar field remains overdamped and its energy almost constant until the attractor is attained. In Fig 3 we assume an abrupt transition from inflation with essentially constant energy to radiation type scaling at scale factor  $a = 1$ , and take the initial fraction of the energy in the scalar field to be  $3 \times 10^{-4}$ . The energy density approaches that in the attractor by  $a \sim 10$ , and then oscillates about it as it approaches it asymptotically. Without

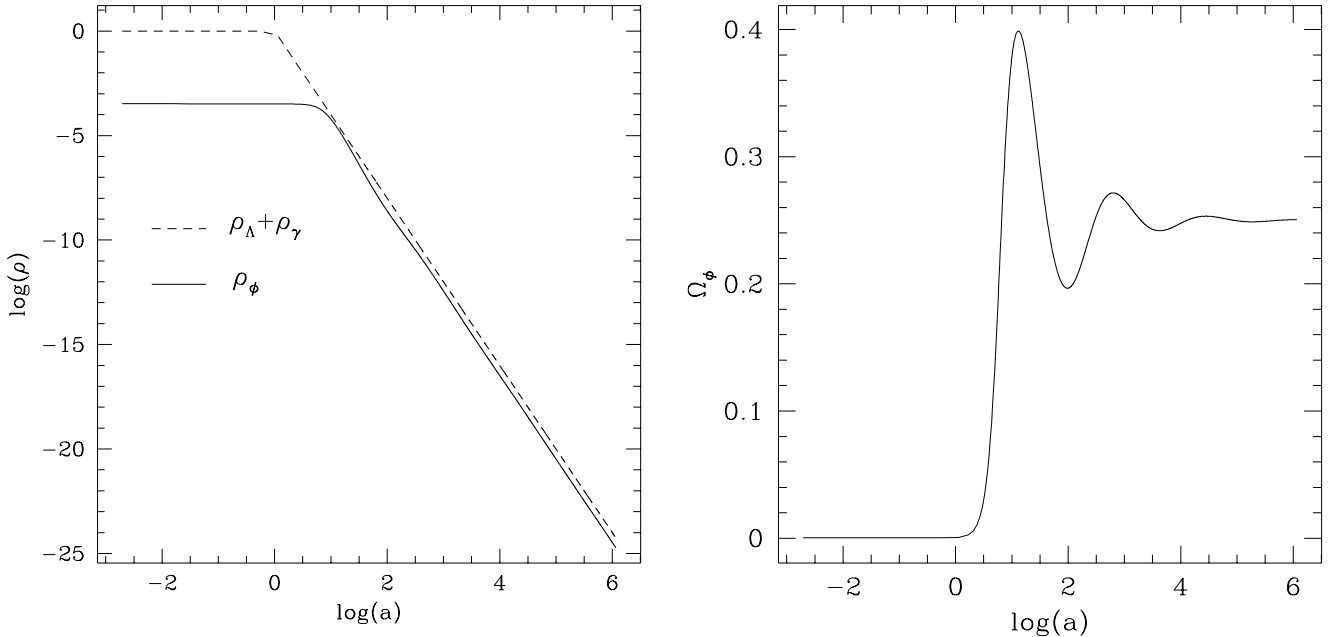


FIG. 3. In the left panel we plot the evolution of the energy density in the scalar field ( $\rho_\phi$ ) with  $\lambda = 4$  and in the remaining matter as a function of scale factor (the units are arbitrary), in the case that the scalar field is initially sub-dominant. In the right panel we plot the evolution of the fractional density in the scalar field.

further detailed analysis it is clear that for a typical inflationary model, in which the reheat temperature is at most a few orders of magnitude below the GUT scale, the attractor will be approached to great accuracy not only by the time scales relevant to structure formation, as we assume below, but also long before nucleosynthesis.

Late entry into the attractor for the scalar field, in particular late in the matter dominated epoch as assumed in the case of this type treated in [18], is therefore certainly not what one would expect from typical inflationary models with the usual method of reheating. Inflation is however not embodied in a specific model or set of models, and it would certainly be possible (and easy to see how) to devise a model in which the energy density in the scalar field at the end of inflation could be tuned to any required value.

Given that the attractor solution is typically established by nucleosynthesis, one must satisfy the constraint discussed above. Converting (17) to one on the contribution from the scalar field at late times (in the matter dominated epoch) gives<sup>2</sup>

$$\Omega_\phi < 0.1 - 0.15 \quad \text{or} \quad \lambda > 5.5 - 4.5 \quad (20)$$

It is because this quantity would seem to be too small to play any important cosmological role that this kind of attractor solution has been disregarded by the authors who have noted these solutions<sup>3</sup>. That this is not in fact the case we will see in greater detail in the later part of this paper. Because the contribution is important for a long time it can have just as significant an effect as a larger contribution which plays a role only at late times.

The initial motivation for our detailed study of this model was not, however, the realization that the attractor might consistently be established by nucleosynthesis for cosmologically relevant cases. Rather our starting point was the observation that there are interesting and viable cosmologies in which scalar field energy in a rapidly scaling mode could dominate over radiation in the very early universe, and that in the case that this field is an exponential of the

<sup>2</sup>The upper bound here which corresponds to the analysis of [41] is actually given explicitly in this form (for the exponential attractor) in [42].

<sup>3</sup>Ratra and Peebles [16] give this explicitly as the reason for the attractor solution model being “phenomenologically untenable” (p. 3416). Wetterich in [20] considers the homogeneous cosmology of the case in which the exponential field dominates at late times; in order to satisfy the nucleosynthesis constraint he discusses the possibility of late entry brought about by a tuning of the initial scalar energy density to an appropriately small value, and also the possibility that  $\lambda$ , rather than being constant, decreases between nucleosynthesis and late times.

type relevant to late time cosmology, there may be, as shown in Fig 1 a transient period between the two epochs (of domination by the scalar field, and the late time attractor) lasting many expansion times in which the scalar field energy is negligible. If this transient period includes nucleosynthesis the constraint (20) would not apply. We now discuss this model and examine how the time of entry into the attractor depends on the parameters in the model.

### F. Late Entry in an Alternative Model of Reheating

An epoch dominated by a scalar field in a mode scaling faster than radiation (or *kination* [44]) comes about by construction in an alternative theory of reheating suggested in [47]. Instead of rolling down to the minimum of a potential, oscillating and decaying, as envisaged in the standard reheating scenario, the inflaton field can roll into a steeper potential supporting a mode scaling faster than radiation (i.e. an exponential with  $\lambda > 2$  or steeper). Rather than being, as is often stated, completely ‘cold and empty’ at the end of inflation, the universe contains a component of radiation created simply by the expansion of the universe (with energy density  $\sim H^4$ ). Although initially very sub-dominant relative to the energy  $\rho_\phi$  in the scalar field ( $H^4/\rho_\phi \sim \rho_\phi/M_P^4$ ) a transition to a radiation dominated cosmology will take place at some subsequent time since the radiation red-shifts away slower than the energy in the scalar field.

We restrict ourselves to the case that the relevant field is the simple exponential with  $\lambda > 2$  (i.e.  $\Omega_\phi < 0.75$ ). We evolve the system of scalar field plus radiation and matter forward in time from the end of inflation, at which time we take the initial conditions to be specified by

$$V(\phi_o) = 3M_P^2 H_i^2 \quad \dot{\phi}_o = 0 \quad \rho_{\text{rad}}^o = \epsilon H_i^4 \quad \epsilon = 10^{-3} \quad (21)$$

where  $H_i$  is the expansion rate at the end of inflation. The initial condition assumes an abrupt end to slow-roll inflation i.e. when the inflaton begins rolling in the region in which the potential is exponential, the potential energy is still dominant. The choice  $\epsilon = 10^{-3}$  corresponds to the simplest estimate of the initial radiation density, taking it to be dominated by the radiation at the horizon scale at the end of inflation (with ‘temperature’  $T \sim H/2\pi$  [46], see [47,45] for a more detailed discussion). We will see below that the results we are interested in here are not very sensitive to these choices.

In this model with the exponential potential there are then just two parameters:  $H_i$ , the expansion rate at the end of inflation, and  $\lambda$  (or, equivalently,  $\Omega_\phi \equiv 3/\lambda^2$  in the attractor in matter domination). These entirely specify the post-inflationary homogeneous cosmology, which evolves, as illustrated in Fig 1, from the scalar field dominated phase through a transient into the late time attractor. What we want to determine here is the time at which the attractor is approached as a function of  $H_i$ , and the range of parameters for which the model is compatible with nucleosynthesis.

The results, which are summarized in Fig 4, can be understood after some closer examination of the solutions. The first feature to note is that the nucleosynthesis constraint, denoted by the hatched region, allows a range of  $H_i$  at given  $\Omega_\phi$  which is (i) only bounded below for  $\Omega_\phi < 0.15$ , (ii) bounded above and below for  $\Omega_\phi > 0.15$  in a range which pinches off as  $\Omega_\phi \rightarrow 0.5$ , so that for larger values of  $\Omega_\phi$  there is no parameter space in the model compatible with nucleosynthesis.

This can be understood as follows. The lower bound comes from the requirement that the initial regime of scalar field dominance end sufficiently long before nucleosynthesis. In its initial phase the scalar field approaches rapidly a mode in which it scales approximately as  $1/a^6$  for  $\Omega_\phi < 0.5$  (or as given by (8) for  $\Omega_\phi < 0.5$  ( $\lambda > \sqrt{6}$ )). In order that the radiation  $\rho_{\text{rad}}^i$  come to dominate by the time its temperature ( $T \sim H_i a_i/a$ ) corresponds to that at nucleosynthesis ( $T_{ns} \sim 1$  MeV), this means (from (21)) that

$$H_i > M_P \left( \frac{T_{\text{end}}}{M_P} \right)^{\frac{1}{2}} \left( \frac{3}{\epsilon} \right)^{\frac{1}{4}} \approx 10^7 \text{ GeV} \quad (22)$$

where  $T_{\text{end}}$  is defined as the temperature at which the scalar field energy becomes equal to that in the radiation, and we took  $T_{\text{end}} = 3$  MeV to obtain the numerical value. The higher value of the lower bound in Fig 4 results from the fact, since our initial conditions are still inflationary, the scalar field takes a short time to attain the rapidly scaling behaviour assumed in deriving (22). The increase of the lower bound with  $\Omega_\phi$  is explained in the same way - the transition to the  $1/a^6$  scaling takes longer as the potential flattens (as  $\lambda$  decreases). From (22) we also can see quantitatively the weak dependence on  $\epsilon$ .

As we observed in Fig 1 the scalar field dominance is followed by a transient period in which it is very sub-dominant, before approaching the late-time attractor. The upper bound on  $H_i$  which appears at  $\Omega_\phi = 0.15$  is just the requirement that, for  $\Omega_\phi > 0.15$  (using the weaker limit of the bound in (17)), this period lasts until after nucleosynthesis. This gives an upper bound because the transient ends earlier according as the first phase of scalar field dominance does. In

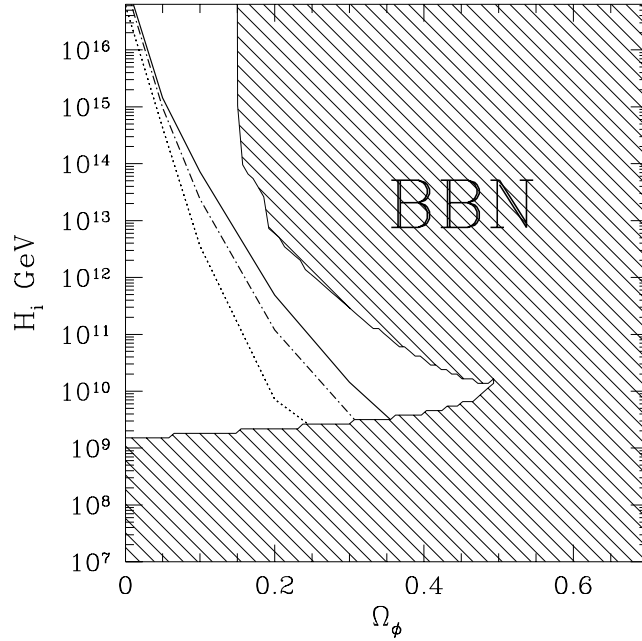


FIG. 4. Reheating by kination in a simple exponential potential: The solid region is that excluded by nucleosynthesis constraints. The solid line (dash-dot, dotted) show the models for which the attractor is established at the beginning of structure formation (matter domination, today).

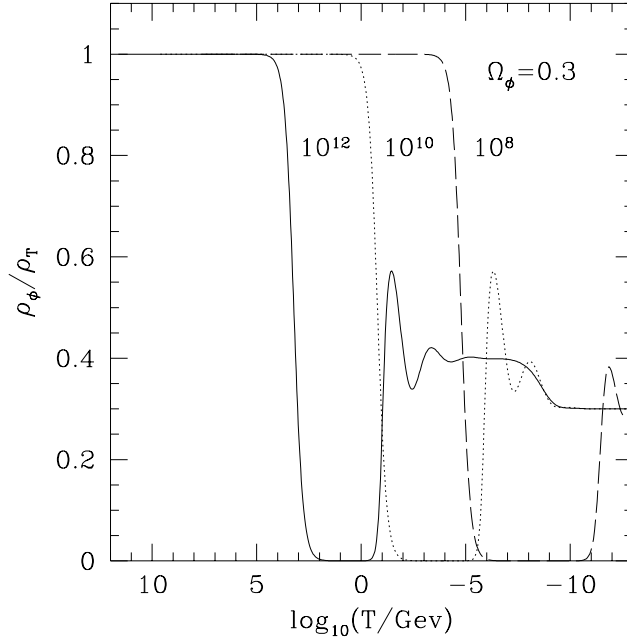


FIG. 5. The fractional energy density as a function of temperature for  $\Omega_\phi = 0.3$  and three values of  $H_i$ .

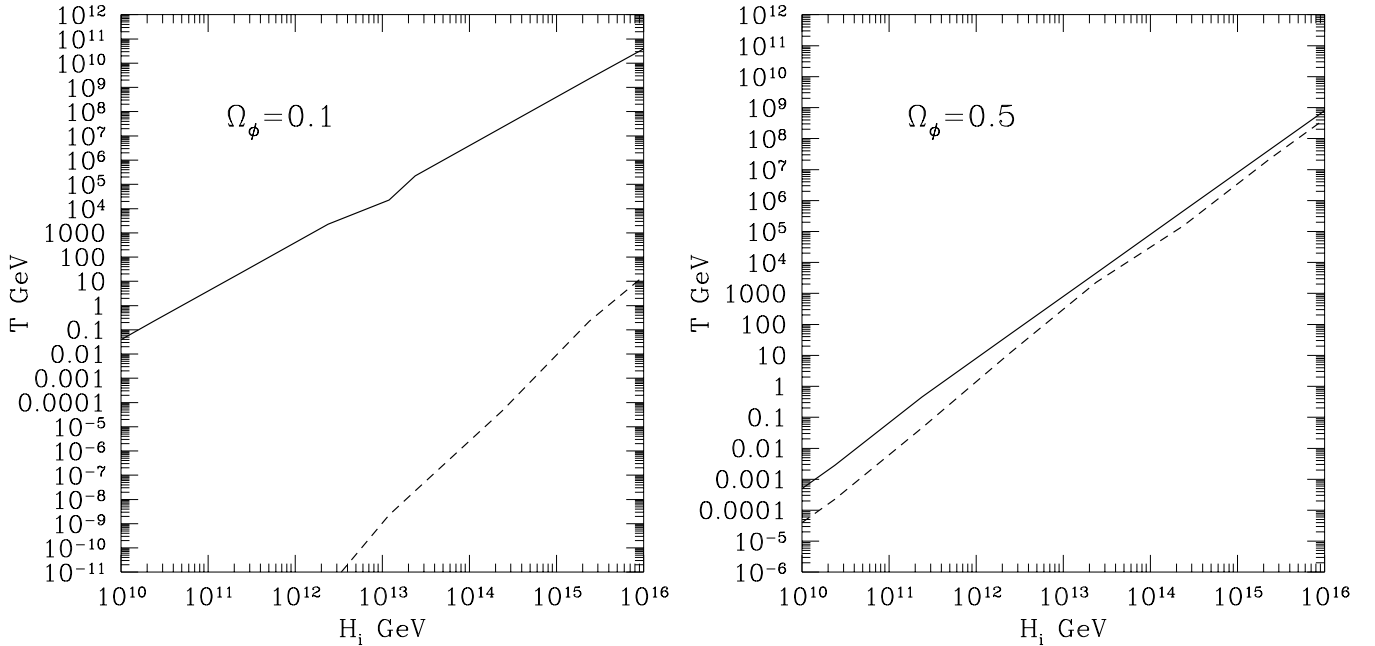


FIG. 6. The solid line is the temperature at which the scalar field energy density first equals that in the radiation and the dashed line is the temperature at which the attractor is established.

Fig 5 we see the evolution of the fraction of the energy density as a function of temperature for various different  $H_i$ . For  $H_i = 10^{12}$  GeV the nucleosynthesis bound is violated because we enter the attractor too early ; for  $H_i = 10^8$  GeV it is violated because we exit the first phase too late. Why the allowed range of  $H_i$  ‘pinches off’ as we go to  $\Omega_\phi = 0.5$  is that the duration of the transient decreases as we approach this value. This can be seen clearly from Fig 6 which show, for  $\Omega = 0.1$  (left panel) and  $\Omega = 0.5$  (right panel) the temperature  $T_{end}$  (when the scalar field energy first equals that in the radiation) and at  $T_{att}$ , when the attractor is established. This behaviour can be understood by looking back to the attractor solutions (8). In the late time attractor the parameter  $\xi = V(\phi)/\rho_\phi$  must reach a certain determined value; as indicated by (8) the value  $\lambda = \sqrt{6}$  separates two quite distinct regions in which  $\xi$  behaves quite differently. For  $\lambda < \sqrt{6}$  the  $\rho_n = 0$  attractor tends to a finite value; in the steeper potential with  $\lambda > \sqrt{6}$  the potential energy ‘runs away’ faster and  $\xi$  decreases rapidly towards zero. As long as  $\xi \approx 0$  the scalar energy continues to scale away as  $1/a^6$ , and it may take a long time for the kinetic energy to catch up again on the potential energy (which essentially stops decreasing once the field’s roll is damped by the radiation or matter). The large ‘undershoot’ and long period of sub-dominance of the scalar energy thus results from the fact that the exponential field with  $\lambda > \sqrt{6}$  evolves for a long time damped only by its own energy density, which allows the field to run away so fast that the potential energy decreases enormously. On the other hand for  $\Omega = 0.6$  ( $\lambda = \sqrt{5}$ ) the scalar field in the first phase follows the  $\rho_n = 0$  attractor (8) with  $\xi = 5/6$ , and only a little adjustment is needed to find the late time radiation dominated attractor with  $\xi = 2/3$ . The nucleosynthesis constraint is therefore never satisfied in this case.

Also shown in Fig 4 are the curves corresponding to ‘entry’ to the attractor at different temperatures - at 100eV (solid line), at matter-radiation equality (dash-dot line) and today (dotted line). The undashed region lying to the right of the first of these lines corresponds to the parameter space (for this model) we will consider in the rest of this paper, which is consistent with nucleosynthesis and with our assumption of the validity of the attractor with (9) as our homogeneous solution. The line corresponding to re-entry at nucleosynthesis is not given, but one can infer that it would mark out a substantial part of this region (bounded by the solid line), which corresponds to entry into the the attractor after nucleosynthesis but prior to  $T = 100eV$ . There is also a region, bounded by the first and third line, which we do not describe and which might be of relevance to late time cosmology. The region to the left of the dotted line corresponds to regions where the scalar field would still be irrelevant today, and therefore the existence of the exponential field has no implications for late time cosmology.

One can also determine from Fig 4 that, for entry in the matter dominated epoch, the largest possible value of  $\Omega_\phi$  in this model is approximately 0.3. This places an upper bound on what contribution to the energy density might be expected to come from this type of solution, if one is not to use the sort of tuning which, as we have emphasised, the model has the merit of being able to avoid. (In particular we note that we cannot obtain the case  $\Omega_\phi = 0.6$  of [18].)

Is there a ‘natural’ value for  $H_i$  within the allowed range?  $H_i$  is related to the inflaton energy at the end of inflation

by  $\rho_i \sim (H_i M_P)^2$ , and the range  $H_i \in [10^8, 10^{16}] \text{ GeV}$  corresponds approximately to  $\rho_i^{1/4} \in [10^{13}, 10^{17}] \text{ GeV}$ . With a more developed model with a full ansatz for the part of the potential which supports inflation, one can relate  $H_i$  to the amplitude of density perturbations, and require that they match those observed in the CMBR by COBE. The simplest calculation (for a very flat inflaton potential) would give  $\rho_i^{1/4} \sim 10^{16} \text{ GeV}$ , or  $H_i \sim 10^{14} \text{ GeV}$ . However the result is not model independent. In [45] a particular model is constructed in which  $H_i$  can be as low as the value at which the phase of scalar dominance ends just before nucleosynthesis. This parameter range for the model has the particular interest that it leads to quite radical modifications of physics at the electroweak scale, since the expansion rate can be up to five order of magnitude greater than in the radiation dominated case at  $T \sim 100 \text{ GeV}$ .

In the rest of this paper we study only cosmology starting from  $T \sim 100 \text{ eV}$ . We will assume the existence of the simple exponential, and take the homogenous cosmology about which we perturb to be given exactly by the attractor at this initial time.  $\lambda$  is thus the sole adjustable parameter additional to those of  $\Lambda \text{CDM}$ . To allow the simplest direct comparison of structure formation in our model with  $\Lambda \text{CDM}$  we take the fiducial value  $\Omega_b h^2 = 0.0125$  for the baryon fraction. In the present study we will not consider the effect of varying this parameter. If we were to do so we would have to be more definite about our assumptions about nucleosynthesis, since the allowed range of  $\Omega_b h^2$  (or equivalently baryon to photon ratio  $\eta$ ) depends on the expansion rate at nucleosynthesis. The canonically quoted range, which corresponds to that consistent with observations for the case  $N_\nu = 3$ , narrows as the expansion rate at freeze-out increases (since the fraction of Helium produced increases as the expansion rate does). As the expansion rate reaches its upper bound, the  $\eta$  required for consistency with observations is pushed towards its lower bound. Having used the constraints of structure formation to determine the best value of  $\Omega_\phi$  in our model, we will comment again in our conclusions on the consistency of entry to the attractor prior to nucleosynthesis.

### III. EVOLUTION OF PERTURBATIONS

We now analyse the evolution of perturbations in this cosmology. The structure of this section is as follows. We firstly write down the equations for the unperturbed cosmology in conformal coordinates which we use in the rest of the paper. For completeness, in III B we present the equations for the evolution of cosmological perturbations in the synchronous gauge. In III C we derive analytic solutions to the evolution of perturbations on sub- and superhorizon scales in the radiation and matter era. It becomes apparent that they are very similar to those in a cosmology in which part of the matter content is in a massive neutrino (MDM). It is thus instructive to identify the key differences between our scenario and the MDM model, and we do so in III D. In III E we look at the evolution of perturbations in the radiation and how it affects the temperature anisotropy angular power spectrum.

#### A. Equations of Motion and Initial Conditions for the Background

Normalising the scalar field in units of  $M_P$  and defining the origin of  $\Phi$  so that the scalar potential is  $M_P^4 e^{-\lambda\Phi}$ , the equation of motion for the unperturbed background scalar field is, in conformal coordinates for which  $ds^2 = a^2[-d\tau^2 + \delta_{ij} dx^i dx^j]$ ,

$$\begin{aligned} \ddot{\phi} + 2\mathcal{H}\dot{\phi} - a^2 \lambda M_P^2 \exp(-\lambda\phi) &= 0 \\ \mathcal{H}^2 &= \frac{1}{3M_P^2} a^2 (\rho_\phi + \rho_M) \end{aligned} \quad (23)$$

where  $a$  is the scale factor,  $\mathcal{H}$  is the conformal Hubble factor, dots denote derivatives with respect to conformal time  $\tau$ ,  $\rho_M$  is the energy density in matter and radiation, and

$$\rho_\phi = M_P^2 \left[ \frac{1}{2a^2} \dot{\phi}^2 + M_P^2 \exp(-\lambda\phi) \right] \quad (24)$$

In the attractor (9) we have

$$\frac{\rho_K}{\rho_\phi} = \frac{n}{6} \quad \frac{\rho_\phi}{\rho_{total}} = \frac{n}{\lambda^2} \quad \rho_{total} = 3M_P^2 \left( \frac{\mathcal{H}}{a} \right)^2 \quad (25)$$

where  $\rho_K = \frac{1}{2a^2} \dot{\phi}^2$  is the kinetic energy density of  $\phi$ . We use these to fix the initial conditions on  $\phi$  and  $\dot{\phi}$  to be

$$\dot{\phi} = \frac{n}{\lambda} \mathcal{H} \quad \phi = -\frac{1}{\lambda} \log \left( \frac{4n(6-n)\mathcal{H}^2}{a^2 \lambda^2} \right) \quad (26)$$

where  $n = 4$ , since we begin the evolution deep in the radiation dominated epoch.

## B. Linear Perturbation Theory

We use the notation and results of Ma & Bertschinger [48], with the modifications brought about by the addition of a scalar field; we present the full set of equations but we refer the reader to [48] and [49] for details on how to solve them. The formalism we work in is the synchronous gauge where  $ds^2 = a^2[-d\tau^2 + (\delta_{ij} + h_{ij})dx^i dx^j]$ . Restricting ourselves to scalar perturbations, the metric perturbations can be parametrised as

$$h_{ij} = \int d^3k e^{i\mathbf{k}\cdot\mathbf{x}} [\hat{\mathbf{k}}_i \hat{\mathbf{k}}_j h(\mathbf{k}, \tau) + (\hat{\mathbf{k}}_i \hat{\mathbf{k}}_j - \frac{1}{3}\delta_{ij})6\eta(\mathbf{k}, \tau)]. \quad (27)$$

Pressureless matter (cold dark matter) has only one non-zero component of the perturbed energy-momentum tensor:

$$\delta T_0^0 = -\rho_c \delta_c \quad (28)$$

and it evolves as

$$\dot{\delta}_c = -\frac{1}{2}\dot{h} \quad (29)$$

Radiation can be characterised in terms of a temperature brightness function,  $\Delta_T(\mathbf{k}, \hat{\mathbf{n}}, \tau)$  and polarization brightness  $\Delta_P(\mathbf{k}, \hat{\mathbf{n}}, \tau)$ . These brightness functions can be expanded in Legendre polynomials of  $\hat{\mathbf{k}} \cdot \hat{\mathbf{n}}$ :

$$\begin{aligned} \Delta_T(\mathbf{k}, \hat{\mathbf{n}}, \tau) &= \sum_{\ell=0}^{\infty} (-i)^\ell (2\ell+1) \Delta_{T\ell}(k, \tau) P_\ell(\hat{\mathbf{k}} \cdot \hat{\mathbf{n}}) \\ \Delta_P(\mathbf{k}, \hat{\mathbf{n}}, \tau) &= \sum_{\ell=0}^{\infty} (-i)^\ell (2\ell+1) \Delta_{P\ell}(k, \tau) P_\ell(\hat{\mathbf{k}} \cdot \hat{\mathbf{n}}). \end{aligned} \quad (30)$$

Defining the density, velocity and shear perturbations by

$$\delta_\gamma = \Delta_{T0} \quad \theta_\gamma = \frac{3}{4}k\Delta_{T1} \quad \sigma_\gamma = \frac{1}{2}\Delta_{T2} \quad (31)$$

the perturbed energy-momentum tensor for radiation is

$$\begin{aligned} \delta T_0^0 &= -\rho_\gamma \delta_\gamma \\ ik^i \delta T_i^0 &= \frac{4}{3}\rho_\gamma \theta_\gamma \\ \delta T_j^i &= \frac{1}{3}\rho_\gamma \delta_\gamma + \Sigma_j^i \\ (\hat{\mathbf{k}}_i \hat{\mathbf{k}}_j - \frac{1}{3}\delta_{ij}) \Sigma_j^i &= -\frac{4}{3}\rho_\gamma \sigma_\gamma \end{aligned} \quad (32)$$

Thomson scattering couples the radiation and baryons, and the latter have a perturbed energy momentum tensor:

$$\begin{aligned} \delta T_0^0 &= -\rho_b \delta_b \\ ik^i \delta T_i^0 &= \frac{4}{3}\rho_b \theta_b \end{aligned} \quad (33)$$

The evolution equations for radiation are:

$$\begin{aligned} \dot{\delta}_\gamma &= -\frac{4}{3}\theta_\gamma - \frac{2}{3}\dot{h} \\ \dot{\theta}_\gamma &= k^2 \left( \frac{1}{4}\delta_\gamma - \sigma_\gamma \right) an_e \sigma_T (\theta_b - \theta_\gamma) \\ 2\dot{\sigma}_\gamma &= \frac{8}{15}\theta_\gamma - \frac{3}{5}k\Delta_{\gamma 3} + \frac{4}{15}\dot{h} + \frac{8}{5}\dot{\eta} \\ &\quad - \frac{9}{5}an_e \sigma_T \sigma_\gamma + \frac{1}{10}an_e \sigma_T (\Delta_{P0} - \Delta_{P2}) \\ \dot{\Delta}_{T\ell} &= \frac{k}{2\ell+1} [\ell \Delta_{T(\ell-1)} - (\ell+1) \Delta_{T(\ell+1)}] - an_e \sigma_T \Delta_{T\ell} \\ \dot{\Delta}_{P\ell} &= \frac{k}{2\ell+1} [\ell \Delta_{P(\ell-1)} - (\ell+1) \Delta_{P(\ell+1)}] \\ &\quad + an_e \sigma_T [\Delta_{P\ell} + \frac{1}{2}(\Delta_{T2} + \Delta_{P0} + \Delta_{P2})(\delta_{0\ell} + \frac{\delta_{5\ell}}{5})] \end{aligned} \quad (34)$$

and for baryons

$$\begin{aligned}\dot{\delta}_b &= -\theta_b - \frac{1}{2}\dot{h} \\ \dot{\theta}_b &= -\mathcal{H}\theta_b + R n_e \sigma_T (\theta_\gamma - \theta_b)\end{aligned}\tag{35}$$

$\sigma_T$  is the Thomson scattering cross section,  $n_e$  is the electron density, and  $R = \frac{4\rho_\gamma}{3\rho_b}$ . The evolution equations for massless neutrinos can be obtained from those for radiation by setting  $\Delta_P = R = \sigma_T = 0$  and  $T \rightarrow \nu$ .

The perturbation  $\varphi$  in the scalar field about the homogeneous solution  $\phi$  has the equation of motion

$$\ddot{\varphi} + 2\mathcal{H}\dot{\varphi} - \nabla^2\varphi + a^2V''\varphi + \frac{1}{2}\dot{\phi}\dot{h} = 0\tag{36}$$

and gives rise to perturbations in the energy momentum tensor which are

$$\begin{aligned}a^2\delta T_0^0 &= -\dot{\phi}\dot{\varphi} - a^2V'\varphi \\ -a^2\partial_i\delta T_i^0 &= \dot{\phi}\nabla^2\varphi \\ a^2\delta T_i^i &= 3\dot{\phi}\dot{\varphi} - 3a^2V'\varphi.\end{aligned}\tag{37}$$

Finally we have the perturbed Einstein equations

$$\begin{aligned}k^2\eta - \frac{1}{2}\mathcal{H}\dot{h} &= 4\pi G a^2 \delta T_0^0 \\ k^2\dot{\eta} &= 4\pi G a^2 i\hat{\mathbf{k}}_i \delta T_i^0 \\ \ddot{h} + 2\mathcal{H}\dot{h} - 2k^2\eta &= -8\pi G a^2 \delta T_i^i \\ \ddot{h} + 6\dot{\eta} + 2\mathcal{H}(\dot{h} + 6\dot{\eta}) - 2k^2\eta &= +24\pi G a^2 (\hat{\mathbf{k}}_i \hat{\mathbf{k}}_j - \frac{1}{3}\delta_{ij})\Sigma_j^i\end{aligned}\tag{38}$$

Having defined the evolution equations for the perturbations, all that remains to be specified are the initial conditions. We are working within the context of inflation and consider an initial set of perturbations of the type generically predicted by the simplest such scenarios: We assume a Gaussian set of adiabatic perturbations with a scale invariant power spectrum. This completely defines the statistical properties of the ensemble. Putting the adiabatic perturbations in the superhorizon growing mode gives [48]:

$$\begin{aligned}\delta_\gamma &= -\frac{2}{3}C(k\tau)^2 \\ \delta_c &= -\frac{1}{2}h = \delta_b = \frac{3}{4}\delta_\nu = \frac{3}{4}\delta_\gamma \\ \theta_\gamma &= \theta_b = \frac{14 + 4R_\nu}{23 + 4R_\nu}\theta_\nu = -\frac{1}{18}(k^4\tau^3) \\ \sigma_\nu &= \frac{4C}{3(15 + 4R_\nu)}(k\tau)^2 \\ \eta &= 2C - \frac{5 + 4R_\nu}{6(15 + 4R_\nu)}C(k\tau)^2\end{aligned}\tag{39}$$

and, as we will see in more detail below,

$$\delta_c = \frac{5\lambda}{4}\varphi\tag{40}$$

(and  $C$  is the overall normalisation). All the remaining perturbation variables are set to zero initially.

### C. Asymptotic solutions to the evolution of density perturbations

We can arrive at a simple understanding of how perturbations evolve in this scenario by considering the simplified case in which there is only cold dark matter, radiation and the scalar field. The evolution equations are then:



$$\ddot{\delta}_c + \mathcal{H}\dot{\delta}_c - \frac{3}{2}\mathcal{H}^2(\Omega_c\delta_c + 2\Omega_r\delta_r) - 2\dot{\phi}\dot{\varphi} + a^2V'\varphi = 0 \quad (41)$$

$$\ddot{\delta}_r + \frac{1}{3}k^2\delta_r - \frac{4}{3}\ddot{\delta}_c = 0 \quad (42)$$

$$\ddot{\varphi} + 2\mathcal{H}\dot{\varphi} + k^2\varphi + a^2V''\varphi - \dot{\phi}\dot{\delta}_c = 0 \quad (43)$$

where  $\Omega_X = \rho_X/\rho_{tot}$  ( $X = C, \gamma, \nu, \phi$ ).

Consider first the superhorizon evolution. In this limit we set  $k^2 = 0$  and (assuming adiabatic initial conditions as above)  $\delta_c = \frac{3}{4}\delta_\gamma$ . Using the scaling solutions for the homogeneous mode of the scalar field, in the radiation era we have:

$$\begin{aligned} \ddot{\delta}_c + \frac{1}{\tau}\dot{\delta}_c - \frac{4(1-\frac{4}{\lambda^2})}{\tau^2}\delta_c - \frac{8}{\lambda\tau}\dot{\varphi} - \frac{4}{\lambda\tau^2}\varphi &= 0 \\ \ddot{\varphi} + \frac{2}{\tau}\dot{\varphi} + \frac{4}{\tau}\varphi - \frac{4}{\lambda}\dot{\delta}_c &= 0 \end{aligned} \quad (44)$$

These equations are solvable and give  $\delta_c$  and  $\varphi$  as a linear combination of  $\tau^2$ ,  $\tau^{-2}$  and  $\tau^{\frac{-1 \pm \sqrt{-15+64/\lambda^2}}{2}}$ . Taking only the coefficient of the growing mode to be non-zero, we find (as stated above)  $\delta_c = \frac{5\lambda}{4}\varphi = A\tau^2$ . On superhorizon scales in the matter era we have

$$\begin{aligned} \ddot{\delta}_c + \frac{2}{\tau}\dot{\delta}_c - \frac{6(1-\frac{3}{\lambda^2})}{\tau^2}\delta_c - \frac{12}{\lambda\tau}\dot{\varphi} - \frac{18}{\lambda\tau^2}\varphi &= 0 \\ \ddot{\varphi} + \frac{4}{\tau}\dot{\varphi} + \frac{18}{\tau}\varphi - \frac{6}{\lambda}\dot{\delta}_c &= 0 \end{aligned} \quad (45)$$

which can be solved to give  $\delta_c$  and  $\varphi$  as a linear combination of  $\tau^2$ ,  $\tau^{-3}$  and  $\tau^{\frac{-6 \pm \sqrt{-7+12/\lambda^2}}{4}}$ . With the assumption therefore of initial adiabatic perturbations in the growing mode in the radiation era, we have  $\delta_c = \frac{28\lambda}{6}\varphi \propto \tau^2$ . We conclude, therefore, that the evolution of perturbations on superhorizon scales are exactly the same as in a scalar field free universe. This is just a manifestation of the fact that, on very large scales, the dominant interaction is gravitational, which is blind to matter type.

Next we turn to the subhorizon evolution of perturbations, i.e.  $k\tau \gg 1$ . Consider first the radiation era. Assuming that the gravitational feedback is unimportant on small scales, we have

$$\begin{aligned} \ddot{\delta}_c + \frac{1}{\tau}\dot{\delta}_c - \frac{3(1-\frac{3}{\lambda^2})}{\tau^2}\delta_\gamma - \frac{8}{\lambda\tau}\dot{\varphi} - \frac{4}{\lambda\tau}\varphi &= 0 \\ \ddot{\delta}_\gamma + \frac{1}{3}k^2\delta_\gamma &\simeq 0 \\ \ddot{\varphi} + \frac{2}{\tau}\dot{\varphi} + k^2\varphi &\simeq 0 \end{aligned} \quad (46)$$

The last two equations are easy to solve, giving  $\delta_\gamma \propto e^{\pm \frac{ik}{\sqrt{3}}\tau}$  and  $\varphi \propto \frac{1}{\sqrt{\tau}}J_{\frac{1}{2}}(k\tau)$ ,  $\frac{1}{\sqrt{\tau}}N_{\frac{1}{2}}(k\tau)$  where  $J_\mu$  and  $N_\mu$  are spherical Bessel functions. Clearly these have little effect on  $\delta_c$  and one can drop these terms from the first equation to get  $\delta_c \propto C_1 \log \tau$ . The subhorizon evolution in the radiation era is thus essentially the same in a universe with and without a scalar field.

In the matter era on sub-horizon scales the equations reduce to

$$\ddot{\delta}_c + \frac{2}{\tau}\dot{\delta}_c - \frac{6(1-\frac{16}{3\lambda^2})}{\tau^2}\delta_c - \frac{12}{\lambda\tau}\dot{\varphi} - \frac{18}{\lambda\tau^2}\varphi = 0 \quad (47)$$

$$\ddot{\varphi} + \frac{4}{\tau}\dot{\varphi} + k^2\varphi - \frac{6}{\lambda\tau}\dot{\delta}_c = 0 \quad (48)$$

To a first approximation we can discard the gravitational feedback term in Eq. 48. The solutions to this wave equation are  $\varphi \propto \frac{1}{\tau^{3/2}}J_{\frac{3}{2}}(k\tau)$ ,  $\frac{1}{\tau^{3/2}}N_{\frac{3}{2}}(k\tau)$  i.e. oscillatory solutions with decaying amplitudes. Clearly this will contribute little to the growing mode and we can drop the last two terms in Eq. 47. The equation is easy to solve and, using  $\Omega_\phi = \frac{3}{\lambda^2}$  we find the growing mode solution  $\delta_c \propto \tau^{2+\frac{5}{2}(-1+\sqrt{1-\frac{24}{25}\Omega_\phi})}$ . The subhorizon growing mode is therefore suppressed relative to that in a scalar field free universe.

Having derived these approximate forms we now have a rough idea of what the mass variance per unit in  $\ln k$  is, where this is defined as

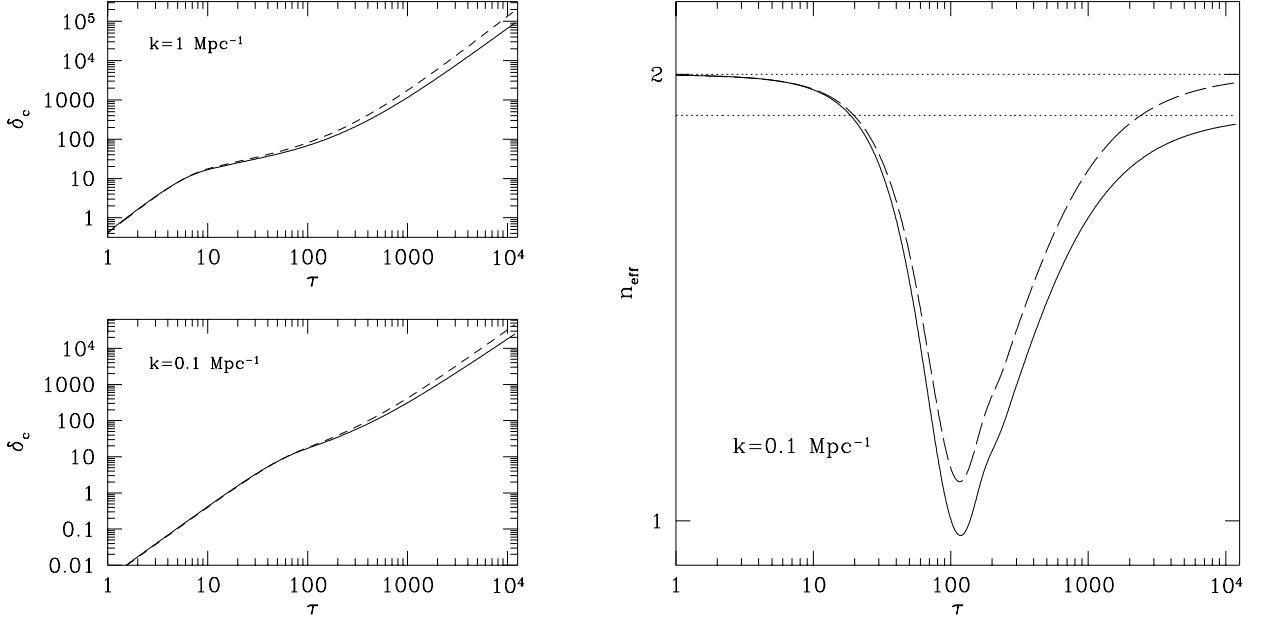


FIG. 7. On the left panel we plot the evolution of  $\delta_c$  for two wavenumbers in a  $\Lambda$ CDM cosmology (dashed line) and in a universe with  $\Omega_\phi = 0.1$ . In the right panel we plot  $n_{eff}$  for  $k = 0.1 \text{Mpc}^{-1}$  for the same cosmology. The upper (lower) dotted line is the asymptotic matter era solution in the  $\Lambda$ CDM ( $\Omega_\phi = 0.1$ ) case.

$$\Delta^2(k) = \frac{k^3}{2\pi^2} \langle |\delta_c(k)|^2 \rangle. \quad (49)$$

One has (defining  $2\epsilon = 5(-1 + \sqrt{1 - \frac{24}{25}\Omega_\phi})$ )

$$\Delta^2(k) \propto \begin{cases} k^4 & \text{if } k \leq \frac{2\pi}{\tau_0} \\ k^{4-2\epsilon} & \text{if } k \leq \frac{\tau_{eq}}{2\pi} \\ \text{constant} + \ln k & \text{if } k > \frac{\tau_{eq}}{2\pi} \end{cases} \quad (50)$$

It is instructive to see the evolution of density perturbations for a few wavenumbers, one that comes into the horizon at around radiation-matter equality ( $k = 0.1 \text{Mpc}^{-1}$ ) and one that comes in during the radiation era ( $k = 1.0 \text{Mpc}^{-1}$ ) for  $\Omega_\phi = 0.1$ . They are compared in Fig 7 to density perturbations in a universe with no scalar field and it is clear that there is a suppression of growth after horizon crossing. Another useful quantity to plot is the dimensionless growth rate  $n_{eff} = \frac{\tau}{\delta_c} \dot{\delta}_c$ . For a scalar field free universe we know that deep in the radiation or matter era  $n_{eff} = 2$ . For the scalar field cosmology we have deep in the radiation era  $n_{eff} = 2$  but deep in the matter era  $n_{eff} = 2 - \epsilon$ . In Fig 7 we plot  $n_{eff}$  for  $k = 0.1 \text{Mpc}^{-1}$  and can clearly see the different asymptotic regimes. Note that there is a long transient to the matter era solution in both the cosmologies considered.

#### D. A comparison with the evolution of perturbations with mixed dark matter

By analysing the simplified system we have been able to get an idea of what to expect from solving the full set of perturbation equations. We found that the presence of  $\phi$  in the matter era suppressed the growth of perturbations by an easily determined factor. The behaviour of this system is very much like that of an MDM cosmology. There one has, in addition to pressureless matter, radiation, baryons and massless neutrinos, a component of matter in two species of massive neutrinos with masses,  $m_\nu$  of order a few eV. The evolution of the energy density is similar to that of the scalar field in the present case. Deep in the radiation era, these neutrinos behave as a massless species and therefore the energy density scales as radiation ( $\propto 1/a^4$ ), while deep in the matter era they behave as non-relativistic matter which scales as  $1/a^3$ . Unlike the scalar field case, where the transition between the two regimes is determined by the transition from radiation to matter domination the transition in the case of the neutrinos occurs when  $3k_B T_\nu \simeq m_\nu$ , where  $k_B$  is the Boltzmann constant and  $T_\nu$  is the massive neutrino temperature. This corresponds to redshift

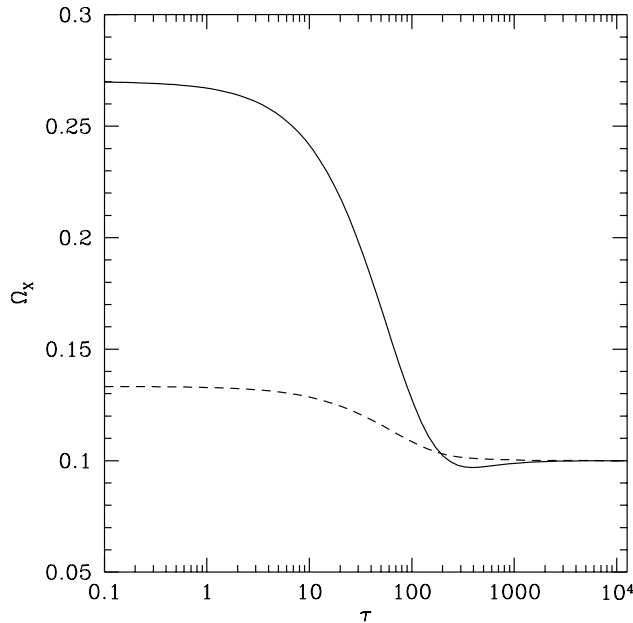


FIG. 8. The evolution of the fractional energy density in  $\phi$  (dashed line) for a  $h = 0.5$  universe with  $\Omega_\phi = 0.1$ ,  $\Omega_c = 0.85$  and  $\Omega_b = 0.05$  and the fractional energy density in two species of massive neutrinos (solid line) with  $\Omega_\nu = 0.1$  (massive),  $\Omega_c = 0.85$  and  $\Omega_b = 0.05$ .

$z \simeq 1.8 \times 10^5 \frac{m_\nu}{30\text{eV}}$ . In Fig 8 we plot the evolution of the energy densities in the extra component in each of the two cosmologies. The energy density in the scalar field  $\phi$  follows the transition very tightly while the energy density in neutrinos becomes non-relativistic after radiation-matter equality. In the latter case there is a short period of time after equality when the massive neutrinos contribute less to the energy density than they do asymptotically, and as a result the pressureless matter clumps more strongly for this period.

The correction to the exponent of the growing mode in the matter era is also very similar in the two models. In [50] it was shown that the correction for MDM is  $\epsilon_\nu = \frac{5}{2}(-1 + \sqrt{1 - \frac{24}{25}\Omega_\nu})$ , exactly the same as we have just derived for the scalar field cosmology. The reason is just that the sole assumption in the derivation of this result was that the exotic form of matter (the  $\phi$  field in our case and the massive neutrinos in the MDM case) does not cluster below a certain scale. There is however again a small but important difference. For  $\varphi$ , the scale below which a given mode does not cluster is the horizon, i.e.  $\propto \frac{1}{\tau}$ . Once it comes into the horizon it *never* clusters. For the massive neutrino perturbations this is not the case. The free-streaming scale, when the neutrinos are non-relativistic is  $k_{fs} = 8a^{1/2}(m_\nu/10\text{eV})h\text{Mpc}^{-1}$ , which *grows* with time. Perturbations of a given wave number  $k$  are damped while  $k > k_{fs}$ , but as soon as  $k_{fs}$  becomes small enough they behave like perturbations in pressureless matter and grow. So perturbations in an intermediate range of wavenumbers, despite suppression during a finite period of time, catch up on the pressureless matter perturbations and contribute to gravitational collapse. This effect can be seen when we compare  $n_{eff}$  for both these scenarios for  $k = 1\text{Mpc}$  (i.e. a mode that comes into the horizon at radiation-matter equality). In Fig 9 we see that, while in the  $\phi\text{CDM}$  case  $n_{eff} \rightarrow \epsilon$ , in the MDM case, perturbations in massive neutrinos start to grow as pressureless matter and  $n_{eff} \rightarrow 2$ .

A further subtle difference between the two scenarios can be seen at the transition between super- and subhorizon behaviour in the radiation era. As shown above, the subhorizon evolution of  $\delta_c$  is  $\propto \text{constant}, \ln \tau$ . The initial amplitude of these solutions is set by the amplitude at horizon crossing, i.e. when  $k\tau \simeq 1$ . In the MDM case, the analysis is also simple. The neutrinos are effectively massless and therefore behave exactly like radiation. So again the subhorizon evolution of  $\delta_c$  is  $\propto \text{constant}, \ln \tau$ . However the transition to subhorizon evolution happens at smaller scales than for the  $\varphi$ . Indeed from the equations we see that the transition should happen when  $c_s k\tau \simeq 1$  (where  $c_s^2 = \frac{1}{3}$ ). A simple way of seeing this is by looking at the source term for the  $\delta_c$  in the radiation era,  $4\mathcal{S}(k, \tau) = \ddot{\delta}_c + \frac{1}{\tau}\dot{\delta}_c = \partial_\tau(\tau n_{eff})\frac{\delta_c}{\tau^2}$ . On superhorizon scales  $\mathcal{S}(k, \tau) = 1$ , and the time when this quantity starts to deviate from a constant indicates the transition from super- to subhorizon behaviour. We have

$$\mathcal{S}(k, \tau) = \frac{3}{4}\mathcal{H}^2(\Omega_\gamma\delta_\gamma + \Omega_\nu\delta_\nu) \quad (51)$$

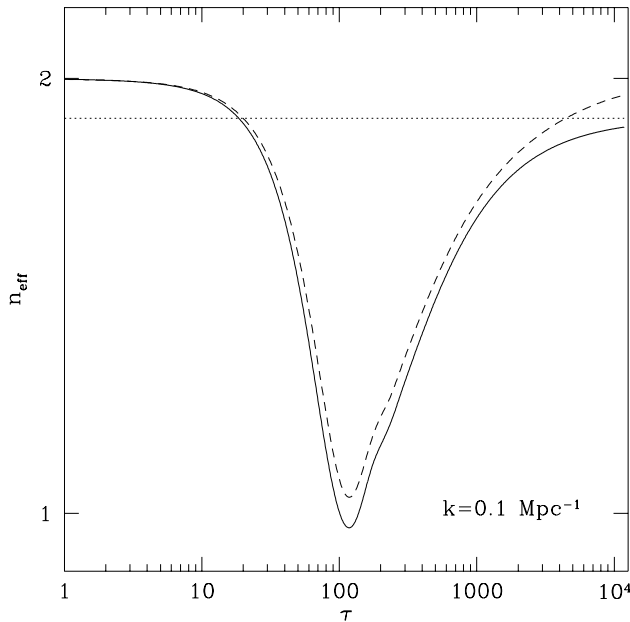


FIG. 9. We plot the evolution of  $n_{eff}$  for  $k = 0.1 \text{ Mpc}^{-1}$  in a MDM cosmology (dashed line) and in a universe with  $\Omega_\phi = 0.1$  (solid line). The dotted line is the asymptotic matter era solution,  $\epsilon$ .

in the MDM scenario where we have grouped the massless and massive neutrinos together, and we have

$$\mathcal{S}(k, \tau) = \frac{3}{4} \mathcal{H}^2 (\Omega_\gamma \delta_\gamma + \Omega_\nu \delta_\nu) + \frac{2}{\lambda \tau} \dot{\phi} + \frac{1}{2\tau^2} \phi \quad (52)$$

in the  $\phi$ CDM case. In Fig. 10 we look at the time evolution of a mode with  $k = 5h \text{ Mpc}^{-1}$  and see that transition to subhorizon evolution occurs earlier in the scalar field scenario than in the MDM scenario. As a result  $\delta_c$  stops growing earlier and there is an additional small, but non-negligible suppression factor in the radiation era.

In Fig. 11 we compare the evolution of  $\delta_c$  for these two models. It is evident that the suppression of  $\delta_c$  in the scalar field model starts much earlier than in the MDM model. This is also clear when we compare  $n_{eff}$  in the two cases.

In conclusion, all these effects we have just discussed combine to give additional suppression in the  $\phi$ CDM model as compared to the MDM model.

### E. The temperature anisotropy angular power spectrum

To complete our analysis of the evolution of perturbations in this cosmology, we shall now look at the effect of the scalar field on the cosmic microwave background. The temperature anisotropy measured in a given direction of the sky can be expanded in spherical harmonics as

$$\frac{\Delta T}{T}(\mathbf{n}) = \sum_{lm} a_{\ell m} Y_{\ell m}(\mathbf{n}) \quad (53)$$

We work again in the framework of inflationary cosmologies so the  $a_{\ell m}$ s are Gaussian random variables which satisfy

$$\langle a_{\ell' m'}^* a_{\ell m} \rangle = C_\ell \delta_{\ell' \ell} \delta_{m' m} \quad (54)$$

The angular power spectrum,  $C_\ell$ , contains all the information about the statistical properties of the cosmic microwave background. One can relate it to the temperature brightness function we derived above through

$$C_\ell = 4\pi \int \frac{dk}{k} |\Delta_{T_\ell}(k, \tau_0)|^2 \quad (55)$$

where we assume again that we are considering the scale-invariant, inflationary scenario.

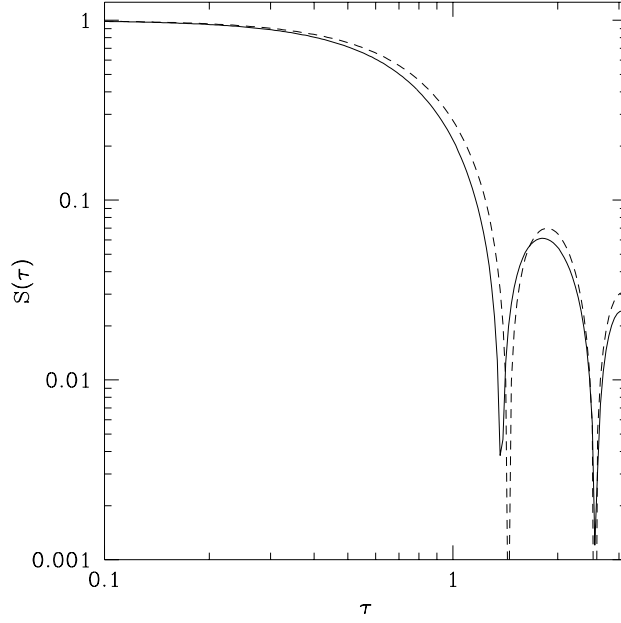


FIG. 10. The evolution of  $\mathcal{S}$  at horizon crossing ( $k = 5h\text{Mpc}^{-1}$ ) for the scalar field cosmology (solid line) and for the mixed dark matter cosmology (dashed line).

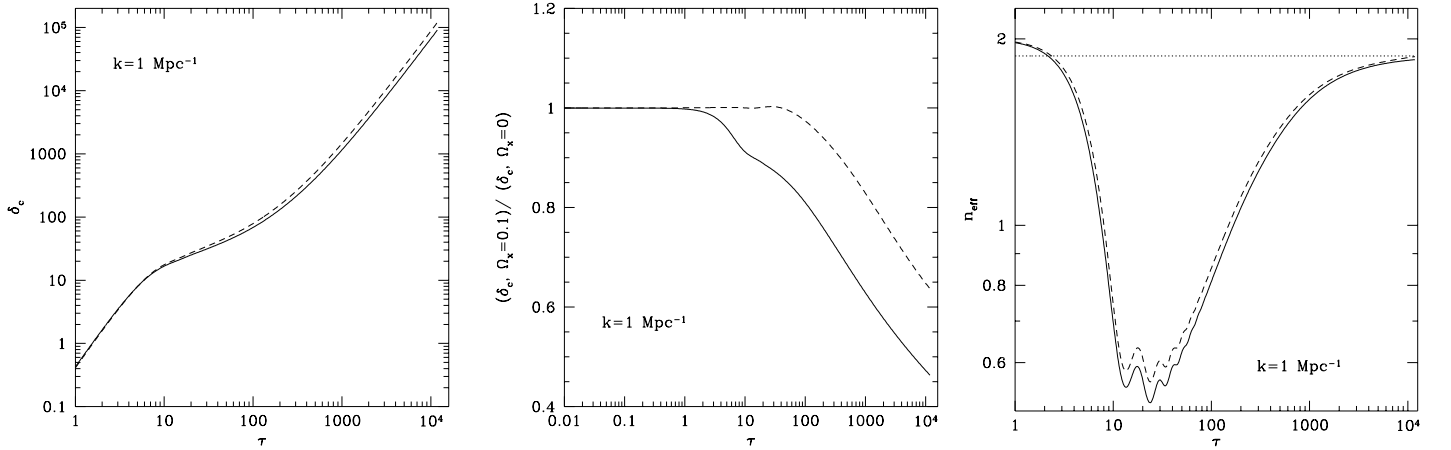


FIG. 11. In the left panel we plot the evolution of  $\delta_c$  ( $k = 1\text{Mpc}^{-1}$ ) for the scalar field cosmology (solid line) and the mixed dark matter cosmology. In the center panel we plot the suppression factor relative to the standard cold dark matter scenario. In the right panel we plot the dimensionless growth rate for these two modes.

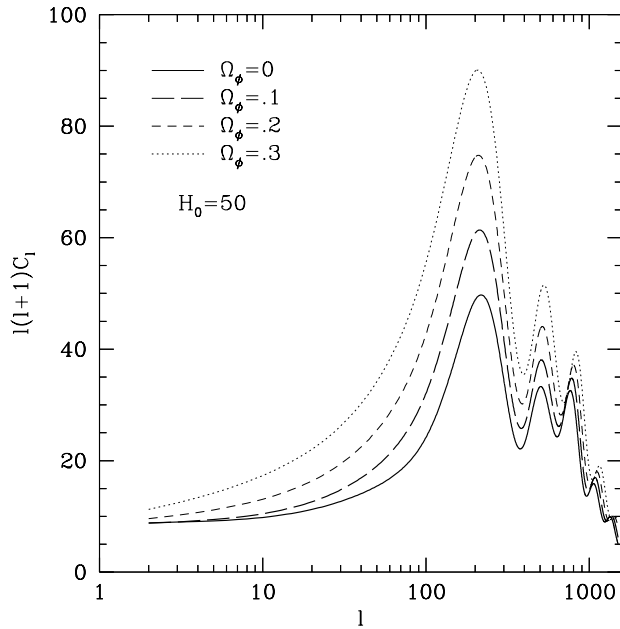


FIG. 12. The angular power spectrum of CMB anisotropies for different values of  $\Omega_\phi$ . These power spectra are not normalised to COBE.

In ref [52], the authors presented a useful simplification with which one can understand the various features in the angular power spectrum. We shall present a simplified version, in the synchronous gauge and use it to understand the effect  $\Omega_\phi$  will have on the  $C_\ell$ s. To a reasonable approximation we can write (defining  $\chi = \frac{\dot{h}+6\dot{\eta}}{2k^2}$ )

$$\begin{aligned} \Delta_{T\ell}(k, \tau_0) = & \left[ \frac{1}{4}\delta_\gamma + 2\dot{\chi} \right] (k, \tau_*) j_\ell(k(\tau_0 - \tau_*)) \\ & + \left[ \frac{\theta_b}{k^2} + \chi \right] \left[ \frac{\ell}{2\ell+1} j_{\ell-1}(k(\tau_0 - \tau_*)) - \frac{\ell+1}{2\ell+1} j_{\ell+1}(k(\tau_0 - \tau_*)) \right] \\ & + \int_{\tau_*}^{\tau_0} (\dot{\eta}(k, \tau) + \ddot{\chi}(k, \tau)) j_\ell(k(\tau_0 - \tau)) \end{aligned} \quad (56)$$

assuming instantaneous recombination at  $\tau_*$  (we do not consider Silk damping in this discussion).

In Fig 12 we plot the angular power spectrum of the CMB for a few values of  $C_\ell$ . Comparing to a  $\Lambda$ CDM  $C_\ell$  we see two effects. Firstly, for  $\ell > 200$  we see that the peaks are slightly shifted to smaller scales. In [51] a clear analysis was presented which explains the location of the peaks in the MDM model scenario, and we will now see that the same effect is present here, *albeit in the opposite direction*. The anisotropies at these scales are generated primarily at  $\tau_*$  and for the purpose of this discussion we can assume that the first term in (56) dominates. As shown in [52] the peak structure of this term is given by

$$\frac{1}{4}\delta_\gamma + 2\dot{\chi} \propto \cos kr_s(\tau_*) \quad (57)$$

where  $r_s$  is the sound horizon in the baryon-photon fluid,  $r_s(\tau) = \int_0^\tau \frac{d\tau'}{3[1+R(\tau')]}$ . Now one of the effects described in [51] and which we see here is that for a given redshift (during a period of time which contains the time of recombination),  $r_s$  is different in the presence of the scalar field than in its absence. This is to be expected as deep in the radiation era we now have three components contributing, the radiation (whose energy density is set by  $T_{CMB}$ , the massless neutrinos (whose energy density is set by  $T_\nu$ ) and the scalar field whose energy density is a constant fraction of the total energy density. Therefore, for a given redshift, the total energy density in the presence of the scalar field is larger than the total energy density in the absence of the scalar field. As a consequence the expansion rate will be larger and the conformal horizon will be smaller. In Fig. 13 we plot the ratio of energy densities and the ratio of comoving horizons as a function of scale factor. At recombination ( $a \simeq 10^{-3}$ ), the conformal horizon (and consequently the sound horizon) is smaller, and as seen in Fig. 12 the peaks are shifted to the right.

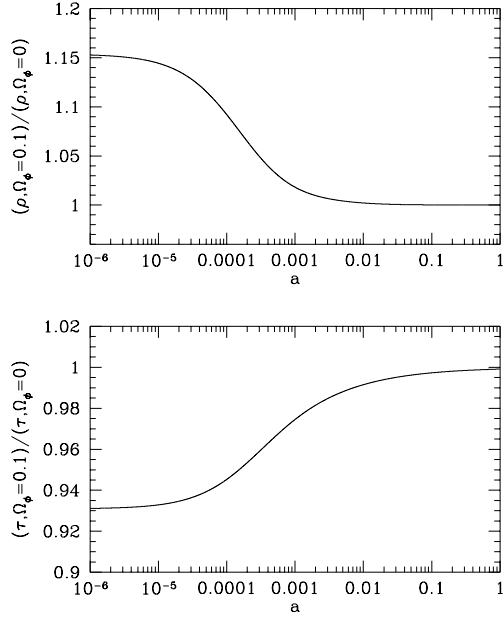


FIG. 13. The top panel shows the ratio of the total energy density in a universe with  $\Omega_\phi = 0.1$  to that in a scalar field free universe. The bottom panel shows the ratio of conformal horizons.

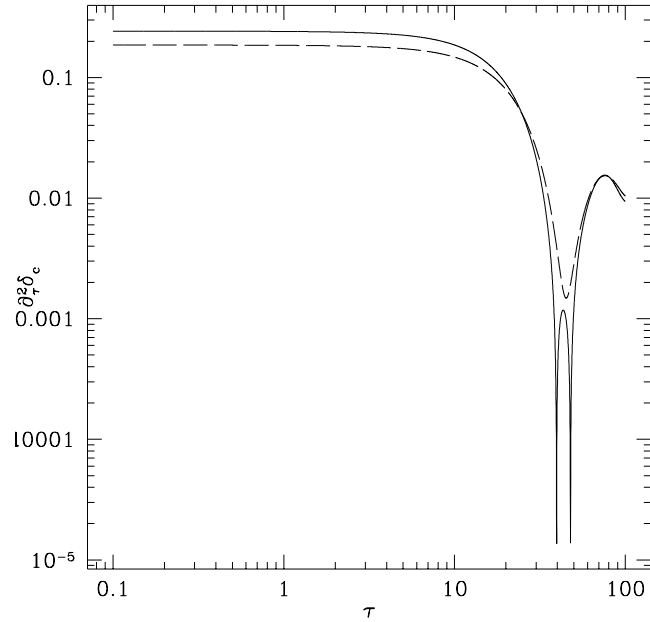


FIG. 14. A comparison of the source of acoustic oscillations in  $\delta_\gamma$  for  $k = 0.2 \text{hMpc}^{-1}$  for SCDM (dashed) and  $\phi\text{CDM}$  (solid) with  $\Omega_\phi = 0.1$  and  $H_0 = 50 \text{Kms}^{-1} \text{Mpc}^{-1}$ .

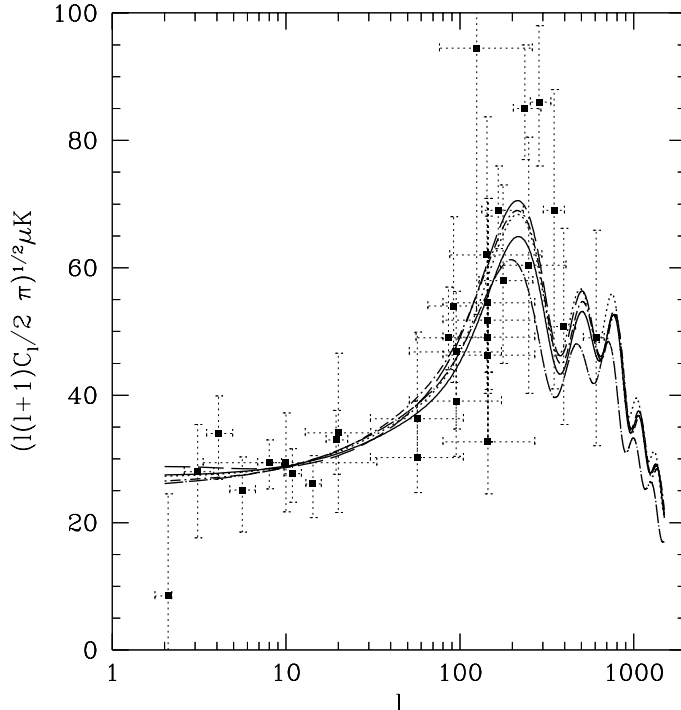


FIG. 15. A comparison of the angular power spectra of temperature anisotropies for five COBE normalized models with the current experimental situation. The models are sCDM in solid, ( $h = .5$ ),  $\Lambda$ CDM in long dash, ( $\Omega_\Lambda = .6$ ,  $h = .65$ ), MDM in dotted, ( $\Omega_\nu = .2$  and  $h = .5$ ),  $\phi$ CDM in dot-short dash, ( $\Omega_\phi = .08$ ,  $h = .5$ ) and  $\phi$ CDM in dot-long dash, ( $\Omega_\phi = .12$ ,  $h = .65$ ). All of them have  $\Omega_b h^2 = 0.0125$ .

Finally, the other effect  $\Omega_\phi$  has on the peaks is to boost their amplitude. Let us assume  $c_s^2 = \frac{1}{3}$ , i.e. we are deep in the radiation era. As shown in the section III C we can write

$$\ddot{\delta}_\gamma + \frac{k^2}{3}\delta_\gamma = \frac{4}{3}\ddot{\delta}_c \quad (58)$$

so the acoustic oscillations are sourced by  $\ddot{\delta}_c$ . One finds that this source is larger in the presence of the scalar field than in its absence (see Fig. 14). The increase in the amplitude of this driving term will increase the amplitude in  $\delta_\gamma$  and lead to the increase by a few percent of the acoustic peaks of the angular power spectrum.

#### IV. CONSTRAINTS FROM COBE AND LARGE SCALE STRUCTURE

In the previous section we have discussed in some detail the evolution of density perturbations and temperature anisotropies in the  $\phi$ CDM cosmology. This approximate analysis indicated that results should be similar to those in the MDM model, except that there should be additional suppression of power in  $\Delta^2(k)$  on small scales. Using the full results of our numerical evolution we now compare our model with the observational constraints which measure fluctuations on a wide range of scales. We first compare the  $C_\ell$ s to the COBE data and calculate the normalization of the perturbations model for different  $\Omega_\phi$ . For completeness we plot a selection of  $C_\ell$  compared to a compilation of data sets and other candidate theories. We then compare  $\Delta^2(k)$  with the observational  $\Delta^2(k)$  rendered in [7] from a compilation of surveys. For this section we define  $\phi$ CDM<sub>1</sub> to be a universe with  $\Omega_\phi = 0.08$ ,  $H_0 = 50\text{kms}^{-1}\text{Mpc}^{-1}$  and  $\phi$ CDM<sub>2</sub> to be a universe with  $\Omega_\phi = 0.12$ ,  $H_0 = 65\text{kms}^{-1}\text{Mpc}^{-1}$ .

The past five years has seen a tremendous growth in experimental physics of the CMB. Over twenty experimental groups have reported detections of fluctuations in the CMB and a rough picture is emerging of the angular power spectrum. It is fair to say that the most uncontroversial and useful measurement that we have is that of COBE, which tells us that on scales larger than  $10^\circ$  the fluctuation are approximately scale invariant with a  $Q_{rms} = 18\mu K$ . Measurements on smaller scales seem to indicate a rise in the power spectrum, but a convincing constraint is still



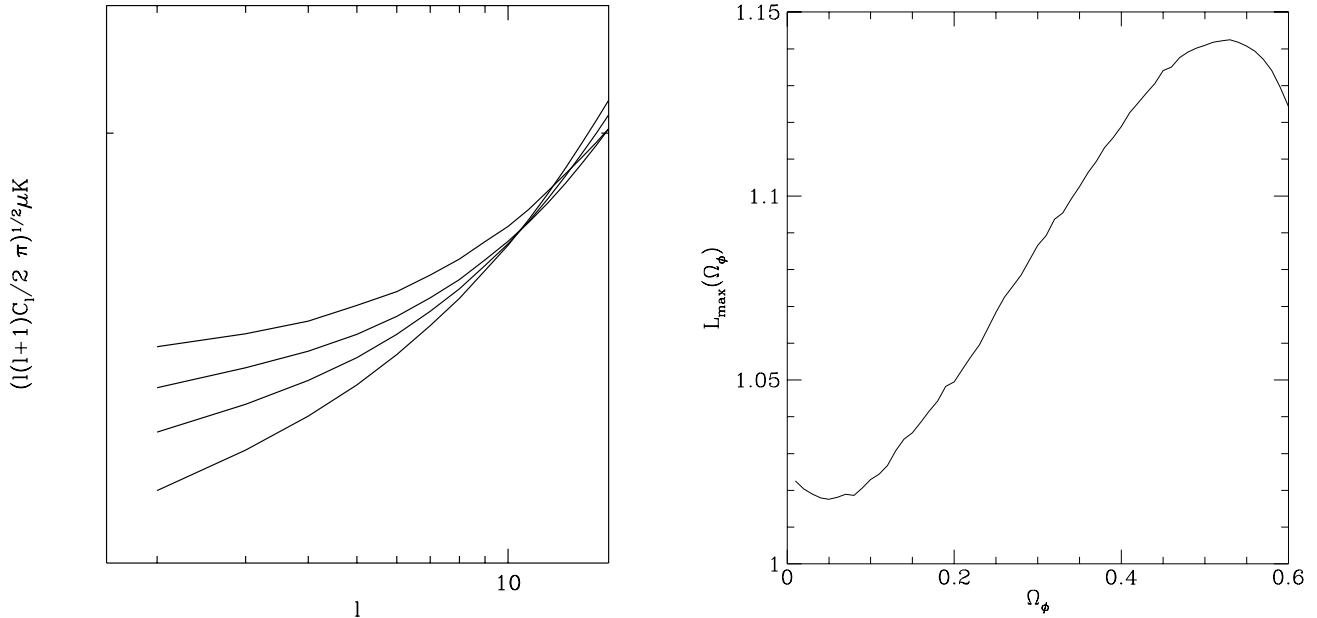


FIG. 16. The left panel shows the small  $\ell$  angular power spectrum for a family of  $\phi$ CDM models. The models are  $\Omega_\phi = 0, 0.04, 0.08$  and  $0.12$  in order of increasing “tilt”. The right panel shows the maximum likelihood of the best fit model as a function of  $\Omega_\phi$ . We have fixed  $h = 0.5$  and  $\Omega_b h^2 = 0.0125$ .

lacking. In Fig 15 we present a compilation of measurements of [53] as compared to two  $\phi$ CDM models and a few candidate rival models. Clearly there is still a large spread although an overall shape is emerging.

In the previous section we described the effect that  $\Omega_\phi$  would have on the  $C_\ell$ s. For small  $\ell$ s the dominant effect to note is the increase in power of the acoustic peaks relative to the large-scale, scale-invariant plateau. The larger is  $\Omega_\phi$ , the larger is the boost and therefore the smaller the  $\ell$ s which are affected. In practice it introduces an effective “tilt” in the large angle power spectrum as can be seen in Fig 16. It is useful to quantify how good a fit  $\phi$ CDM  $C_\ell$ s are to the COBE data. The correct framework to work with is maximum likelihood analysis. In [54] the authors have supplied us with an efficient way of evaluating the likelihood of a given model relative to purely scale invariant fluctuations. On the left panel we plot the likelihood of the best fit model as a function of  $\Omega_\phi$ . There are two important things to note. Firstly the well known fact that, if one includes the quadrupole, the COBE data favours more tilted models and therefore a larger  $\Omega_\phi$ . Secondly, the likelihood function for  $\Omega_\phi$  should be very flat; indeed the dependence of the tilt on  $\Omega_\phi$  is very weak. As explained in the previous section the effect of  $\Omega_\phi$  on the  $C_\ell$ s is of order a few percent and concentrated at large  $\ell$ s. There will be little variation on COBE scales.

One of the key observational constraints for any class of models is the mass variance per unit interval in  $\ln k$  as defined in Eq. 49. This quantifies the amount of clustering over a range of scales. In [7] the authors compiled a series of surveys and attempted to extract what they believe to be the underlying  $\Delta^2(k)$  of the linear density field. This involved a series of corrections: Firstly, the assumption that the different samples were biased in different ways with respect to the underlying density field; secondly, that there are redshift distortions in the observed structures; and finally, that some of the structures have undergone non-linear collapse. This final correction is model dependent and in principal great care should be taken in making definitive comparisons between our theoretical  $\Delta^2(k)$  and that presented in [7]. In practice we shall assume that possible corrections are small and compare them. In a future publication we shall analyse the non-linear features of this theory.

In Fig. 17 we plot a family of COBE normalized  $\Delta^2(k)$  with  $h = 0.5$  and  $\Omega_b h^2 = 0.0125$ . We clearly see the features described in III B, i.e. the larger the  $\Omega_\phi$ , the smaller the  $k$  for which  $\Delta^2(k)$  departs from scale invariance. In the other panel we can also see how it differs from a MDM model with the same background cosmological parameters. For the same energy density in exotic matter component (i.e.  $\phi$  or massive  $\nu$ ) there is more suppression in the  $\phi$ CDM case. Finally we see how it compares to the data of [7]. We find that, for  $\Omega_\phi$  in the range  $0.08 - 0.12$  we can match the data with as good agreement as the MDM model and some other candidate models. This is displayed in Fig 18. In the following table we tabulate the  $\chi_2$  values (with 15 degrees of freedom) of these models, in increasing goodness of fit.  $\phi$ CDM is competitive with the best fit model of MDM.

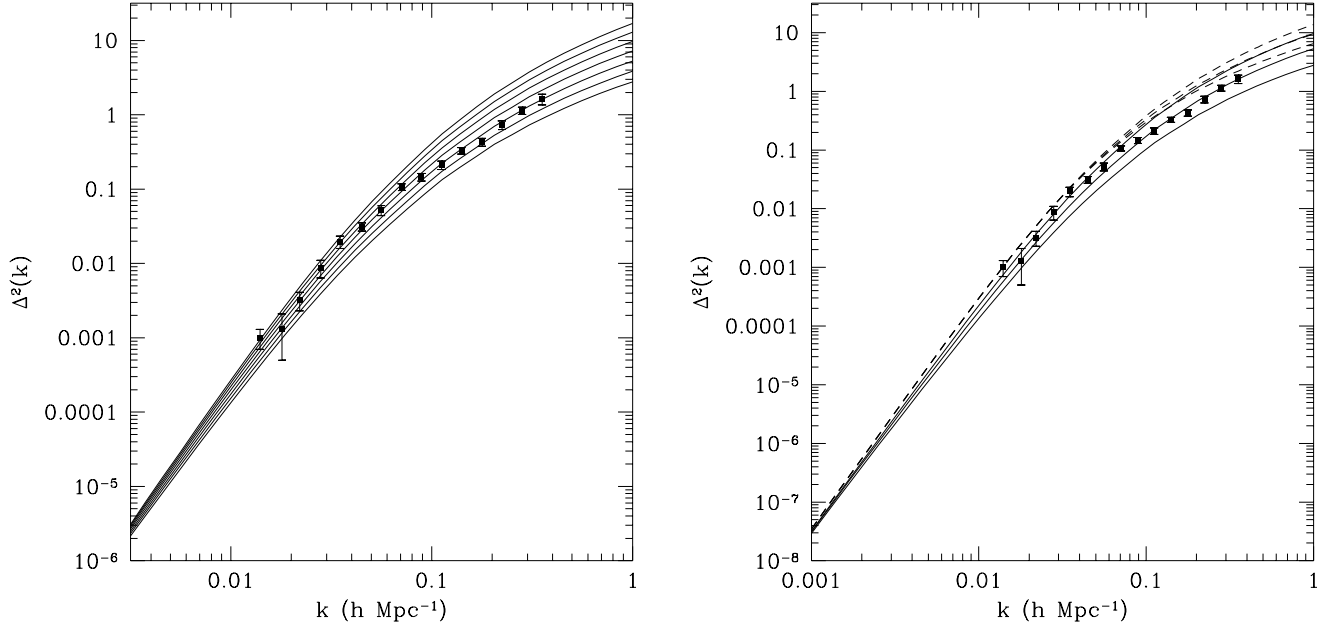


FIG. 17. On the left panel we plot the dependence of  $\Delta^2(k) = \frac{d\sigma^2}{d \ln k}$  on  $\Omega_\phi$ . For  $h = .5$ ,  $\Omega_b h^2 = 0.0125$  we show (in order of decreasing amplitude) plots for  $\Omega_\phi = 0, .02, .04, .06, .08, .10$  and  $.12$ . In the right panel we compare a family of MDM models (dashed, with  $\Omega_\nu = 0.04, 0.08$  and  $0.12$  in order of decreasing amplitude) with a family of  $\phi$ CDM models (dashed, with  $\Omega_\phi = 0.04, 0.08$  and  $0.12$  in order of decreasing amplitude).

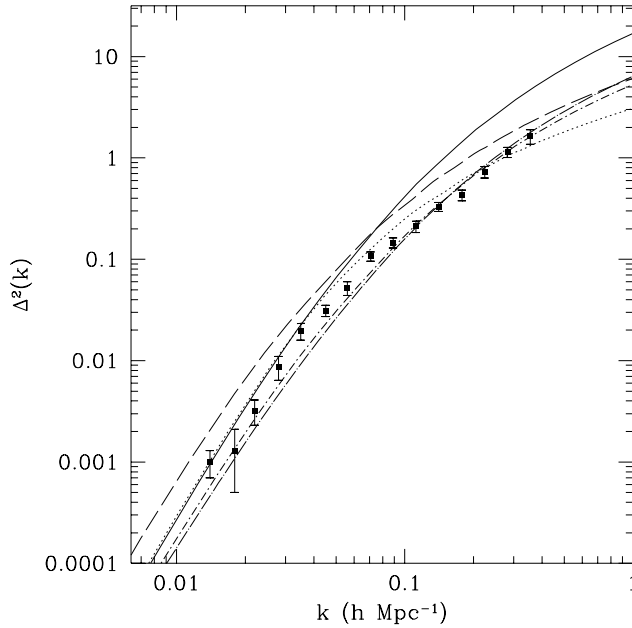


FIG. 18. A comparison of the mass variance per unit interval in  $\ln k$ ,  $\Delta^2(k) = \frac{d\sigma^2}{d \ln k}$ , for five COBE normalized models with a rendition of the linear power spectrum from various data sets (corrections for non-linearity, redshift distortions and biasing have been introduced). The models are sCDM in solid ( $h = .5$ ),  $\Lambda$ CDM in long dash ( $\Omega_\Lambda = .6$ ,  $h = .65$ ), MDM in dotted ( $\Omega_\nu = .2$  and  $h = .5$ ),  $\phi$ CDM in dot-short dash ( $\Omega_\phi = .08$ ,  $h = .5$ ) and  $\phi$ CDM in dot-long dash ( $\Omega_\phi = .12$ ,  $h = .65$ ). All of them have  $\Omega_b h^2 = 0.0125$ .

SCDM	103.96
$\Lambda$ CDM	52.5
$\phi$ CDM <sub>2</sub>	14.5
MDM	10.25
$\phi$ CDM <sub>1</sub>	7.53

One can fit  $\Delta^2(k)$  for these models (to 10% in the range  $0 \leq \Omega_\phi \leq 0.16$ ) with:

$$\Delta^2(k) = D(k, \Omega_\phi) \Delta^2(k)_{CDM}$$

$$D(k, \Omega_\phi) = (1 + 1.5\Omega_\phi - 10\Omega_\phi^2) \left( \frac{1 + 5k^{1.1295} + 4k^{2.259}}{1 + 1 \times 10^7 k^{2.259}} \right)^{1.15\Omega_\phi^{1.01}} \quad (59)$$

where  $\Delta^2(k)_{CDM}$  is the COBE normalized CDM mass variance, and contains all the dependence on remaining cosmological parameters such as  $H_0$  and  $\Omega_b$  [55].

A useful quantity to work with is that characterising the mass fluctuations on  $Rh^{-1}$ Mpc scales

$$\sigma^2(R) = \int_0^\infty \frac{dk}{k} \Delta^2(k) \left( \frac{3j_1(kR)}{kR} \right)^2. \quad (60)$$

In particular it has become the norm to compare this quantity at  $8h^{-1}$ Mpc with the abundances of rich clusters. It is premature to use this constraint with our current understanding of  $\phi$ CDM. The best measurements of such abundances involve an estimate of the number density of X ray clusters of a given surface temperature. To relate these temperatures to masses in an accurate way one has to rely on N-body simulations of clusters. This has been done for a few cosmologies and we can use the results they use as a rough guide but care should be taken with using such results at face value. The fact that we can fit  $\Delta^2(k)$  to the data of [7] is already strong indication that we are on the right track. If we use the values of [58] we have  $\sigma_8 \simeq 0.5 - 0.8$ . A good fit to  $\sigma_8$  is

$$\sigma_8(\Omega_\phi) = e^{-8.7\Omega_\phi^{1.15}} \sigma_8^{CDM} \quad (61)$$

where  $\sigma_8^{CDM}$  is the COBE normalized sCDM  $\sigma_8$ . As would be expected, for the range of values for which we get a good agreement with [7], we also match the cluster abundance constraints.

Finally it is desirable to make a comparison with some measure of small scale clustering at early times. In [59], the authors used a simple analytic estimate of the fraction of collapsed objects at redshift  $z = 3$  and  $z = 4$  to show that for  $\Omega_\nu = 0.3$ , MDM models predict too little structure as compared to that inferred from the Lyman- $\alpha$  measurements [60]. More recently in [61], the authors considered a larger range of cosmological parameters and found that constraints from the Lyman- $\alpha$  systems could be sufficiently restrictive to rule out a large range of models. From Fig 18 we can see that  $\phi$ CDM should fare better than MDM on very small scales. This is easy to understand: We argued in Section III that effectiveness of  $\phi$ CDM was mainly due to the fact that the scalar field free-streaming scale grows with time while the massive neutrino free streaming scale decays with time. We then need a larger amount of massive neutrinos to fit both COBE and the cluster abundances in the MDM model than the amount of scalar field in  $\phi$ CDM. On much smaller scales (the scales probed by Lyman- $\alpha$  systems) i.e. scales smaller than the massive neutrino free streaming scale, perturbations in MDM should be more suppressed than in  $\phi$ CDM. This means  $\phi$ CDM should fare better than MDM with regards to the Lyman- $\alpha$  constraints. A preliminary check on our model can be done using the technique of [59]. In brief one can make a conservative estimate that a fraction  $f_{gas}$  of matter is in gas at that time and set bounds on the amount of objects with masses greater than  $10^{10}(1 - \Omega_\phi)^{-1}h^{-1}M_\odot$ . Using the Press-Schechter formalism one can then derive a bound:

$$\text{erfc}\left(\frac{1.7}{\sqrt{2}\sigma(R, z)}\right) > 0.16h/f_{gas} \quad z = 3$$

$$\text{erfc}\left(\frac{1.7}{\sqrt{2}\sigma(R, z)}\right) > 0.104h/f_{gas} \quad z = 4 \quad (62)$$

where erfc is the complementary error function and  $R = 0.1 - 0.2$ Mpc. For  $\phi$ CDM in the range of  $h$  and  $\Omega_\phi$  that we have been considering we find that if  $f_{gas} = 1$ , these models are consistent with this constraint. Note that the MDM model already has serious problems with this conservative constraint. If we consider a less a conservative constraint and take  $f_{gas} \sim 0.1$  as seems to be indicated by hydrodynamical studies, than  $\phi$ CDM is inconsistent with these measurements. More detailed observations and modeling of Lyman- $\alpha$  systems will supply us with a very strong constraint on this class of models.

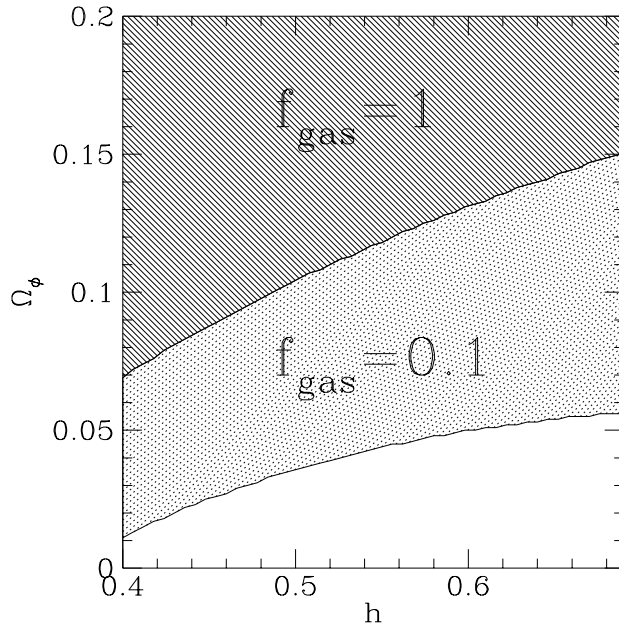


FIG. 19. The shaded region represents the allowed region of parameter space consistent with the Lyman- $\alpha$  constraints of [60]. The solid hatched region corresponds to the values of  $h$  and  $\Omega_\phi$  excluded for  $f_{gas} = 1$ . The dotted hatched region corresponds to the values of  $h$  and  $\Omega_\phi$  excluded for  $f_{gas} = 0.1$ .

## V. CONCLUSIONS

In the first part of this paper we gave the motivation for considering the particular scalar field cosmology we have now studied in detail: The addition made to the standard  $\Lambda$ CDM model does not involve any tuning of the type involved in other modifications, in that no energy scale characteristic of the universe at recent epochs is invoked. The form of the required potential is one which arises in many particle physics models, with values of the single free parameter of the order required. Having analysed the model and determined the best fit to structure formation, we now first comment on these aspects of the model.

In Section II E we argued that, in typical inflationary models with the usual mechanism of reheating, one would expect the attractor solution to be established well prior to nucleosynthesis. In this case we should therefore compare our best fit to the constraint from the latter, as given in (20), which is satisfied (clearly for the conservative bound, and marginally for the tighter one). Further, in this case we need to check that the value  $\Omega_b h^2 = 0.0125$  which is equivalent to the baryon to photon ratio  $\eta_{10} = 3.3$  (in units of  $10^{-10}$ ) is within the allowed range at the corresponding expansion rate. This is not a question which is easy to answer simply because most nucleosynthesis calculations give results only in terms of the range of  $\eta_{10}$  allowed at the standard model expansion rate, or the maximum additional number degree of freedom allowed. For the conservative criteria [41,43] which gave the weaker upper bound in (20) the allowed range narrows from  $\eta_{10} \in [1.65, 8.9]$  at  $\Omega_\phi = 0$  to the lower bound  $\eta_{10} = 1.65$  at  $\Omega_\phi = 0.15$ . Extrapolating the use of these criteria for a more restrictive case for which the required data is given in [42] (i.e. the allowed range of  $\eta_{10}$  is given as a function of the energy density in an extra component) the value  $\eta_{10} = 3.3$  would appear to be in the allowed range at  $\Omega_\phi = 0.1$ . For a more restrictive set of nucleosynthesis constraints a slightly lower value of  $\Omega_b h^2$  might be required for consistency.

In an alternative model of reheating (which is by construction associated with the existence of this same type of potential), we saw that the time of re-entry to the attractor could be after nucleosynthesis, at a time which depends on both  $\Omega_\phi$  and the other parameter in this model  $H_i$ , the expansion rate at the end of inflation. By making the assumption that the attractor is established prior to nucleosynthesis we restricted ourselves to a (large) part of parameter space. From Fig 4 we can read off that this corresponds, for  $\Omega_\phi \approx 0.1$ , to  $H_i > 10^{14} \text{ GeV}$  or  $\rho_i^{1/4} > 10^{16} \text{ GeV}$ . As we noted at the end of section this is consistent with what would guess would be the most natural range of these parameters in this model. On the other hand, it is inconsistent with models in which the phase of scalar field domination continues until just before nucleosynthesis (with the consequences described in [45]) since they correspond to the line defining the lower bound from nucleosynthesis in Fig 4. For entry to the attractor before today, it can be seen from Fig 4 that one requires in this case  $\Omega_\phi > 0.22$ . It would be interesting to analyse the effect on structure

formation in these models, and indeed in all of the parameter space for this model excluded by us in our present analysis.

In terms of  $\lambda$  our best-fit corresponds to the range  $\lambda \in [5, 6.1]$ . As we discussed in Section II B this value is certainly of the order observed in the fundamental particle physical theories of which they have been observed to be a generic feature, and may even be in the precise range found in certain theories. This suggests the exciting possibility of ultimately linking the cosmological features which would provide a signature for these fields to details of physics at the Planck scale. From the point of view of particle physics motivated model-building it would be particularly interesting also to look at models where the simple exponential potential represents the asymptotic behaviour of a potential which can support inflation in another region, since this would be likely to produce a very constrained model (with reheating as discussed).

In Section III we analysed in detail the evolution of perturbations in  $\phi$ CDM. We found that perturbations in the scalar field on subhorizon scales decayed, leading to a suppression of power on small scales. The similarities with MDM led us to pursue the comparison in more detail. We found that the contribution from the scalar field was more efficient at suppressing perturbations in the CDM than massive neutrinos. We showed that this was due to a simple difference in the evolution of the “free-streaming” scale in the two theories: In  $\phi$ CDM the free streaming scale grows with the horizon while in MDM the freestreaming scale decays as  $1/\tau$ . This means that perturbations in the scalar field *never* grow once they come into the horizon, in contrast to perturbations in the massive neutrino which end up clumping after some finite time. We analysed the effect the scalar field would have on the CMB and found it to be small but distinctly different from that of MDM.

In Section IV we used the results of a Boltzmann-Einstein solver to test how well this class of models fared when compared to various astrophysical data. Because of the weak effect the scalar field has on the CMB, the angular power spectrum is effectively (with the current accuracy of experiments) as in SCDM. Using the COBE data we normalized these theories and compared the mass variance per logarithmic interval in  $k$  to the one estimated in [7]. Our models fared as well, or better, than competing flat universe models. A comparison with an estimate of the mass variance at  $8h^{-1}\text{Mpc}$  from the abundances of rich clusters gave the same results. We finally compared the amount of structure at high redshift our model predicts, as compared to that inferred from Lyman- $\alpha$  systems. This has proven to be a serious problem for MDM models. We saw that our model is consistent, albeit marginally, with these constraints.

Lastly a few further comments on other related issues which it would be interesting to investigate:

(i) We assumed an initial flat adiabatic spectrum of perturbations, in line with the most generic type of inflation. Within the context of inflation one can of course have different spectra etc., and within the context of some very well motivated form for the inflationary part of the potential in the alternative reheating model, it would be interesting to look at the combined effect on structure formation. In more general, an interesting feature of the exponential which would be worth investigating is the fact that the attractor is also an attractor for isocurvature fluctuations, and hence the assumption of adiabatic initial conditions might have a much more general motivation than the standard inflationary one.

(ii) Inflation was assumed simply because it is the paradigmatic model. The existence of the exponential scalar field might of course have an effect on any cosmology. In an open cosmology, for example, the analogous attractor also exists in the curvature dominated regime and the asymptotic state has a scalar field energy scaling as  $1/a^2$ .

(iii) We have shown that the effect of the exponential scalar field on the angular power spectrum of the CMB is quite small, much like the case of MDM. However, recent high precision analysis of parameter estimation from the CMB (as one would expect from the satellite missions) indicates that one may achieve a precision of  $\Delta\Omega_\nu=0.04$  or better. This opens up the interesting possibility of actually trying to constrain  $\Omega_\phi$  with the CMB.

(iv) Besides the issue of consistency with entry into the attractor prior to nucleosynthesis which would motivate the study of the dependence on  $\Omega_b h^2$  away from the SCDM value we assumed, there are further observational reasons for doing so. The recent measurements of [62] indicate that one may have a higher baryon content than previously expected. Since a higher baryon content leads to less structure on smaller scales, a best fit to large scale structure constraints would be obtained with a smaller value of  $\Omega_\phi$ . The effect on the Lyman- $\alpha$  constraints might be more dramatic, since there would be a competition between the suppression of power and the increase in the amount of gas simply due to the fact that there are more baryons around. That the result is not immediately evident can be seen from the analysis of MDM in [61]. Further, to determine whether entry to the attractor prior to nucleosynthesis is consistent in this case, one would have to determine whether this decrease in  $\Omega_\phi$  would broaden the allowed range in  $\eta$  sufficiently.

(v) One of the main problems for the MDM model is the overwhelming evidence for structure at high redshift. Critical universe models with massive neutrinos typically underproduce structure as probed by Lyman- $\alpha$  systems and high redshift cluster abundances [64]. This problem is somewhat alleviated in the case of  $\phi$ CDM: The different evolution of the free-streaming scale in  $\phi$ CDM leads to more power on small scales (and consequently high redshifts) relative to MDM. This certainly provides strong motivation for further study of the evolution of perturbations on small scales and high redshift in these models.

From the point of view of structure formation we have described a new model which has the same qualitative features as MDM. Unlike other scalar field cosmologies, which affect the local expansion rate (up to redshift of a few), our background evolution is exactly matter dominated, the modification arising at the perturbation level. Given the wealth of current data on small scales, at recent redshifts, this raises the question of whether this is the right approach to the construction models of structure formation: The existence of structure at high redshift combined with the small scale velocity dispersion today at  $1h^{-1}\text{Mpc}$  seems to argue for a strong modification of the growth rate of perturbations in the last few redshifts. This would point towards a low density universe. However, until we have a more detailed understanding of the non-linear evolution of perturbations in models such as  $\phi\text{CDM}$  (on scales between  $0.1$  and  $10h^{-1}\text{Mpc}$ ), these models should not be ruled out. We are currently analysing the non-linear regime of  $\phi\text{CDM}$  using an N-body code.

ACKNOWLEDGMENTS: We thank C. Balland, M. Davis, J. Levin, A. Liddle, A. Jaffe, T. Prokopec, E. Scanapieco, J. Silk and R. Taillet for useful discussions. P.F. was supported by the Center for Particle Astrophysics, a NSF Science and Technology Center at U.C. Berkeley, under Cooperative Agreement No. AST 9120005. P.F thanks PRAXIS XXI (Portugal) and CNRS (France) for partial support. MJ is supported by an Irish Government (Dept. of Education) post-doctoral fellowship.

- 
- [1] G. Smoot *et al Astroph. Jour.* **4371** 1 (1994)
  - [2] A. Guth *Phys. Rev.* **D23** 347 (1981)
  - [3] A. Linde *Phys. Lett.* **108B** 389 (1982)
  - [4] A. Albrecht and P. Steinhardt *Phys. Rev. Lett* **48**, 1220 (1982)
  - [5] P. Peebles *Principles of Physical Cosmology* PUP, Princeton (1994)
  - [6] S.Dodelson *et al Science* **274** 69 (1996)
  - [7] J. Peacock and S.Dodds *M.N.R.A.S* **267** 1020, 1994
  - [8] S. Carroll, W. Press and E. Turner *A. Rev. Astrophys.* **30**, 499 (1992); J.Ostriker and P. Steinhardt, *Nature* **377** 600 (1995).
  - [9] M.Davis *et al Nature* **359** 393 (1992); A. Taylor and M. Rowan Robinson *Nature* **359** 396 (1992); A. Klypin *et al Astroph. Journ.* **416**, 1 (1993), J. Primack *et al Phys. Rev. Lett* **74** 2160 (1995)
  - [10] J.Gott *Proceedings of Critical Dialogues in Cosmology*, Ed N. Turok, PUP (1996).
  - [11] M. White, G. Gelmini and J. Silk *Phys. Rev.* **D51** 2669 (1995)
  - [12] J. Frieman, C. Hill, A. Stebbins and I. Waga *Phys. Rev. Lett.* **75**, 2077 (1995)
  - [13] K. Coble, S. Dodelson and J. Frieman *Phys. Rev* **D55**, 1851 (1997)
  - [14] M. White, G. Gelmini and J. Silk *Phys. Rev.* **D51** 2669 (1995)
  - [15] A.Vilenkin and P.Shellard *Cosmic Strings and other Topological Defects* CUP 1995; N. Turok *Phys. Rev. Lett* **24** 2625 (1989)
  - [16] B. Ratra and P. Peebles *Phys. Rev* **D37**, 3406 (1988)
  - [17] R.Caldwell *et al astro-ph/9708069*
  - [18] P.Viana and A.Liddle *astro-ph/9708247*
  - [19] P. Ferreira and M. Joyce, *Phys. Rev. Lett.* (1997), to appear, *astro-ph/9707286*.
  - [20] C. Wetterich, *Astron. and Astrophys.* **301**, 321, (1995)
  - [21] E. Copeland, A. Liddle and D. Wands *Ann. N. Y. Acad. Sci* **688** 647 (1993)
  - [22] I.Reid, *Astron. Journ.* **114** 161 (1997); M Feast and R.Catchpole *MNRAS* **286**, L1 (1997); B. Chaboyer, P. Demarque, P. Kernan and L. Krauss *astro-ph/9706128*
  - [23] M. Davis *et al Astroph. Jour.* **473** 22 (1996)
  - [24] A. Dekel *Astron. & Astroph.* **32** 371 (994)
  - [25] Review of Particle Properties, APS (1997)
  - [26] A.Evrard *astro-ph/9701148*
  - [27] M.Turner *Phys. Rev.* **D28** 1243 (1983)
  - [28] J.Halliwell *Phys. Lett.* **B185** 341 (1987).
  - [29] J.Barrow *Phys. Lett* **B187** 12 (1987).
  - [30] F. Lucchin and S. Mattarese *Phys. Rev.* **D32** 1316 (1985).
  - [31] Q. Shafi and C. Wetterich *Phys. Lett.* **B152** 51 (1985)
  - [32] C. Wetterich *Nuc. Phys.* **B252** 309 (1985).
  - [33] Q. Shafi and C. Wetterich *Nuc. Phys.* **B289** 787 (1987)
  - [34] J. Halliwell *Nuc. Phys.* **B266** 228 (1986).

- [35] E.Cremmer *et al Phys. Lett.* **B133** 61 (1983); J. Ellis *et al Phys. Lett.* **B134** 429 (1984); H.Nishino and E.Sezgin *Phys. Lett.* **B144** 187 (1984); E.Witten *Phys. Lett.* **B155** 151 (1985); M.Dine *et al Phys. Lett.* **B156** 55 (1985).
- [36] J.Yokoyama and K.Maeda *Phys. Lett* **B207** 31 (1988)
- [37] Extrapolating the behaviour of these models over such a large range of scales should be done with care. Variations of  $\Delta\Phi > M_P$  are beyond the range in which the approximations we are considering are valid with any accuracy.
- [38] J. Barrow and S. Cotsakis *Phys. Lett.* **B214** 515 (1988).
- [39] S. Cotsakis *Phys. Rev.* **D47** 1437 (1993).
- [40] C. Copi, D. Schramm and M.Turner, *Phys. Rev. Lett* **75** 3981 (1995); B. Fields *et al, New Astronomy* **1** 77 (1996).
- [41] P. Kernan and S. Sarkar, *Phys. Rev.* **D54** 3681 (1996).
- [42] M. Birkel and S. Sarkar, *Astropart. Phys.* **6** 197 (1997).
- [43] S. Sarkar, *Rep. Prog. Phys.* **59**, 1493 (1996).
- [44] M. Joyce, *Phys. Rev.* **D55** 1875 (1997);
- [45] M. Joyce and T. Prokopec, hep-ph/9709320.
- [46] R.Brandenburger and R.Kahn *Phys. Lett* **B119** 75 (1982); R.Brandenburger *Phys. Lett* **B129** 397 (1983).
- [47] B. Spokoiny, *Phys. Lett.***B315** 40 (1993).
- [48] C.P. Ma and E. Bertschinger *Astroph. Jour* **455**, 7, 1995
- [49] U. Seljak and M. Zaldarriaga *Astroph. Jour* **469**, 437, 1996
- [50] J. Bond, G. Efstathiou and J. Silk *Phys. Rev. Lett* **45** 1980, 1980
- [51] S. Dodelson, E. Gates and A. Stebbins *Astroph. Jour* **467**, 10, 1996
- [52] W. Hu and N. Sugiyama *Astroph. Jour* **444**, 489, 1995
- [53] M. Tegmark and A. Hamilton [astro-ph/9702019](http://www.sns.ias.edu/max/cmb/experiments.html); see references in <http://www.sns.ias.edu/max/cmb/experiments.html>
- [54] E. Bunn and M. White *Astroph. Jour.* **480** 6 (1997)
- [55] Note that the BBKS [56] fitting function is not accurate with non-zero baryon content. For this, see [57].
- [56] J. Bardeen *et al Astroph. Jour.* **304**, 15 (1986);
- [57] C.P Ma *Astroph. Jour* **471**, 13, 1996
- [58] S. White, G. Efstathiou C. Frenk *MNRAS* **262**, 1023 (1993)
- [59] A. Liddle *et al, astro-ph/9511057*
- [60] L. Storrie-Lombardi *et al astro-ph/9503089*
- [61] D. Eisenstein and W. Hu [astro-ph/9710252](http://arxiv.org/abs/astro-ph/9710252)
- [62] D. Tytler *et al Nature*, **381**, 207, (1996).
- [63] J.Bond *et al astro-ph/9702100*
- [64] N. Bahcall *et al Astrophys. Jour. Lett* **485** **153** (1997).